In vitro skin models as a tool in the optimization of drug formulation

Zinaida Shakel

Dissertation of the 2nd Year of Studies Conducting the Master's Degree in Biochemistry

This study was conducted under the guidance of Dr. Sofia Teresa Antunes Costa Lima and Prof. Dr. Maria de La Salette de Freitas Fernandes Hipólito Reis Dias Rodrigues

September 2017

Abstract

(Trans)dermal drug therapy is gaining increasing importance in the present-day drug development. To completely use the potential of skin administration, it is important to optimize the delivery of active ingredients/ drugs into/through the skin. The optimization of skin formulations could enhance the desired effect of the therapy and is often included in the early stages of the product development. Currently, most of the optimization is based on the use of appropriate *ex vivo* animal/human models. Alternatives to animals and human skin are impelled by economic and ethical reasons. In this context, the main goals of this study are to develop and characterize a *stratum corneum* model that mimics this human skin layer, inspired on a phospholipid vesicle-based permeation assay.

To mimic the *stratum corneum* layer, the phospholipid vesicles were prepared with a selected lipid composition, which closely corresponds to the main human lipid classes on this skin layer. The design of the developed model was optimized using dynamic light scattering, phospholipid quantification and scanning electron microscopy images. To compare the *stratum corneum* model developed, with the porcine skin model, the storage stability was assessed as well the calcein permeation in the presence of several conditions: a pH range, co-solvents and drugs. The established *stratum corneum* model could be stored at -20°C for up to 2 weeks without significant changes, was stable within the pH range from 2.0 to 8.0 and with the addition of co-solvents (DMSO, cremophor® and oleic acid). Additionally, the model showed a good correlation with the porcine skin model and provided reproducible results regarding the evaluation of the calcein permeability in the presence of some drugs (caffeine, naproxen, diclofenac, methotrexate, cyclosporine).

In sum, the developed *stratum corneum* model allows permeation prognosis when examining drug formulations and can be stably stored. This model can thereby constitute a valuable tool to improve the process of (trans)dermal drugs development, as it may reduce the duration and the economic costs associated, and even replace the animal testing during early stages of drug development.

Keywords: human *stratum corneum*, liposomes, permeability, transdermal drug delivery

Resumo

Atualmente, a administração de tratamentos por via transdérmica tem uma importância crescente no desenvolvimento dos medicamentos. No entanto, de modo a utilizar o potencial da administração através da pele, é importante otimizar a entrega de agentes ativos/ fármacos dentro e/ou através da mesma. A otimização de formulações pretende aumentar o efeito terapêutico pretendido quando aplicado na pele e, é um aspeto avaliado na fase inicial do desenvolvimento do produto. A maior parte da otimização é baseada no uso de modelos animais/ humanos, mas as questões éticas e económicas incentivam a procura de modelos alternativos. Neste contexto, este trabalho de investigação pretendeu desenvolver e caracterizar um modelo de estrato córneo que mimetize esta camada da pele humana, inspirada num ensaio de permeação baseado em vesículas fosfolipídicas.

De modo a mimetizar a camada do estrato córneo, foram preparadas vesículas de fosfolípidos com uma composição lipídica específica baseada nos componentes lipídicos desta camada de pele no Homem. O modelo desenvolvido foi otimizado usando técnicas de dispersão de luz, quantificação de fosfolípidos e microscopia eletrónica de varrimento. Para comparar o modelo de estrato córneo desenvolvido, com o convencional modelo de pele de porco, foram avaliadas: a estabilidade no armazenamento, a taxa de permeabilidade da calceína sozinha e na presença de várias condições (pH 2 a 8, co-solventes e fármacos). Conclui-se que o modelo de estrato córneo desenvolvido pode ser armazenado a -20 °C até 2 semanas sem mudanças significativas relativamente ao seu perfil inicial de permeação, é estável no intervalo de pH de 2,0 a 8,0 e na presença de co-solventes (DMSO, cremophore® e ácido oleico). Além disso, o modelo mostrou uma boa correlação com o modelo de pele de porco e forneceu resultados reprodutíveis quanto à avaliação da permeabilidade da calceína na presença de alguns compostos com potencial terapêutico (cafeína, naproxeno, diclofenac, metotrexato e ciclosporina).

Em resumo, o modelo de estrato córneo desenvolvido permite o prognóstico da permeação de formulações de fármacos e pode ser armazenado de uma forma estável. Assim, este modelo pode constituir uma ferramenta valiosa para melhorar o processo de desenvolvimento de fármacos para via transdérmica e assim reduzir a duração e os custos associados dos tratamentos, e até mesmo substituir os testes em animais durante as primeiras fases de desenvolvimento de fármacos.

Acknowledgements

Firstly, I would like to express my sincere gratitude to my research supervisor Dr. Sofia Lima, for the continuous support of my study and related research, for her patience, motivation, caring, new ideas and immense knowledge. Her guidance helped me in all the time of research and writing of this thesis. I could not have imagined having a better advisor and mentor for this work.

I would also like to show gratitude to Professor Salette Reis, for memorable opportunity to work in her research group, for positive atmosphere, sincere valuable guidance and encouragement extended to me.

I would also like to thank Dr. Cláudia Pinho for her teaching and assistance during lab work, the important suggestions and advices. I have always carried positive memories of her work with me.

I take this opportunity to express gratitude to all my professors in this Master's degree for their help and training.

I would like to thank all members of Laboratório de Química Aplicada, especially to my colleges at Molecular Biophysics and Biotechnology, for their feedback, cooperation and of course friendship. It was fantastic to have the opportunity to work and great sharing laboratory with all of you during this year.

I also thank my family and friends for the support and attention, in particular to my aunt Jekaterina for her financial support and taking care. Finally, I must express my very profound gratitude to Aleksey for providing me with unfailing support and for always believing in me throughout my years of study and through the process of researching and writing this thesis.

This accomplishment would not have been possible without all of you. Thank you so much.

Contents

List of Figures

List of tables

List of abbreviations

5-HT – 5-Hydroxytryptamine

CAMP – Cathelicidin Antimicrobial Peptide

CE – Cornified Envelope

CLE – Corneocyte Lipid Envelope

DLS – Dynamic Light Scattering

DMSO – Dimethylsulphoxide

EPC – Egg L-α-Phosphatidylcholine

FFAs – Free Fatty Acids

GLC – Gas/Liquid chromatography

HEPES – 2-[4-(2-hydroxyethyl)piperazin-1-yl]ethanesulfonic acid hemisodium salt

LUVs – Large Unilamellar Vesicles

MLVs – Multilamellar Large Vesicles

MTX – Methotrexate

Mw – Molecular weight

NHKs – Normal Human Keratinocytes

NMFs – Natural Moisturizing Factors

NMR – Nuclear Magnetic Resonance

NSAIDs – Non-Steroidal Anti-Inflammatory Drugs

OECD – Organization for Economic Co-operation and Development

PAMPA – Parallel Artificial Membrane Permeability Assay

PBS –Phosphate Buffered Saline

PDI – Polydispersity Index

PDMS – Poly(dimethylsiloxane)

PSA – Polar Surface Area

PVPA – Phospholipid Vesicle-based Permeation Assay

S1P – Sphingosine-1-Phosphate

SC – *Stratum Corneum*

SEM – Scanning Electron Microscopy

SUVs – Small Lamellar Vesicles

TDD – Transdermal Drug Delivery

TEER – Transepithelial Resistance

UV – Ultraviolet

VDR – Vitamin D Receptor

I INTRODUCTION

1 Human skin

The skin is the largest organ of the integumentary system, covering about 1.5 – 2 m^2 of the human body surface area and on average calculating for 10% of the body mass for adults.[5, 11] It determines the border between the human body and the external environment, which enables the biological vital functions. Nevertheless, the skin is more than just a physical barrier; it gives an important interface for interaction with the world. Thus, one of its most important roles is to regulate what enters and exits the body. Mainly, the skin is meant for very little penetration, while other tissues, for example the permeable epithelia of the lung and gastrointestinal tract provide the principal sources of regulated entry into the body. Additionally, the skin prevents the body´s dehydration, protects the body against pathogens, enables ultraviolet protection, thermoregulation, sensation, synthesis of vitamin D, and the protection of vitamin B folates. Finally, the skin has highly selective properties and different rate for intake.[3]

The thin outer layer of the epidermis is the *stratum corneum* (*SC*). Generally, it is responsible for the barrier properties of the skin.[12] *SC* is composed of corneocytes (mainly constituted by aggregated keratin filaments covered by a cornified envelope) that are enclosed by extracellular lipids, arranged as multiple lamellar bilayers.[3] These lipid structures prevent excessive loss of water from the organism and block the entry of most topically administered drugs that have high molecular weight and low lipophilicity. Thereby, this barrier represents a great challenge for drug delivery across the skin, intended either for local effects or for systemic therapy.

1.1 Structure of the skin

Skin is a heterogeneous membrane, with hydrophilic properties in an internal layer and lipophilic on its outside area. Each tissue layer is composed of different cell types that have various functions.

There are three structural layers of the skin: the epidermis, the dermis and hypodermis (or subcutis). Moreover, the epidermis can be subdivided into the *stratum corneum* (horny layer), *stratum granulosum* (granular layer), *stratum spinosum* (prickle cell layer) and *stratum basale* (Fig. 1). A complementary layer, the *stratum lucidum* (clear layer) can be found on the palm and sole of the foot, which is responsible for the thickened skin. Nevertheless, the *stratum lucidum* is

often considered the lower part of the *SC* but not an individual epidermal layer. There are also the hair follicles and sweat ducts that cross different skin layers.[5]

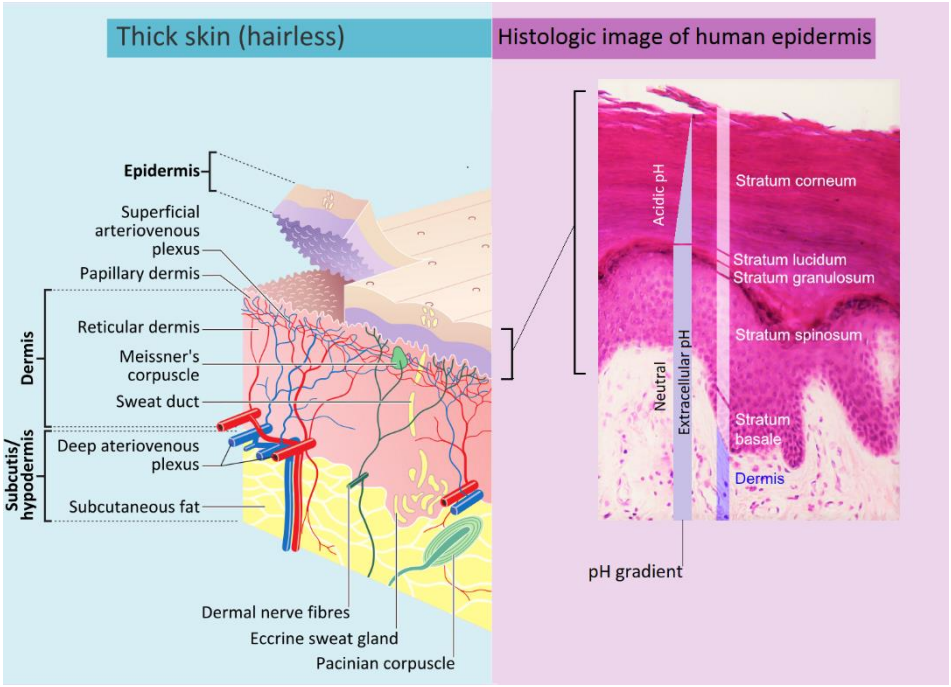

Fig. 1 – Schematic representation of the structure of human skin without hair in cross section and histologic image of the human epidermis (https://commons.wikimedia.org/wiki/File:Epidermal_layers.png#/media/File:Epidermal_layers.png Downloaded July 25, 2017).[1] The extracellular pH of the epidermis remains neutral until the transition between the *stratum granulosum* and *stratum corneum*, where it becomes more acidic towards the surface of the skin [2]

1.1.1 *Stratum Corneum*: structure

The *SC* is a multifunctional outermost layer of the epidermis. The *SC* is typically 10–20 µm thick and composed of 10–15 layers of corneocytes, denucleated forms of keratinocytes, for normal human skin on the body (on the palm and sole about 200 layers) embedded in a lipid matrix.[4, 5] Differences in the layers are a function of body site and reflect the thickness, content of protein (filaggrin)and corneodesmosomes and packing of keratin filaments.[3] The lipid layers, compose the permanent pathway through the *SC* and are indicated as the main barrier for diffusion of substances through the skin.[13]

Corneocytes are lifeless cells obtained from terminally differentiated keratinocytes, during the passage from granular layers to *SC*. This process is characterised by loss of nuclei and cytoplasmic organelles, flattening and elongation of the keratinocytes. Morphological dimension of the corneocytes are about 0.2 µm thick and 40–60 µm wide.[5, 14] Their membrane is 0.015 to 0.020 µm thick and includes involucrin and keratolinin (structural proteins).[8]

The organisation of the *SC* is usually compared with the "bricks and mortar" model (Fig. 2). The bricks are the corneocytes (filled with keratin filaments, dried out, non-living skin cells that are ready to shed). The extracellular matrix analogous to the mortar in a brick wall, which is composed of lipids (stacked lipid bilayers that surround the corneocytes) like the cement holding the bricks together.[3, 4]

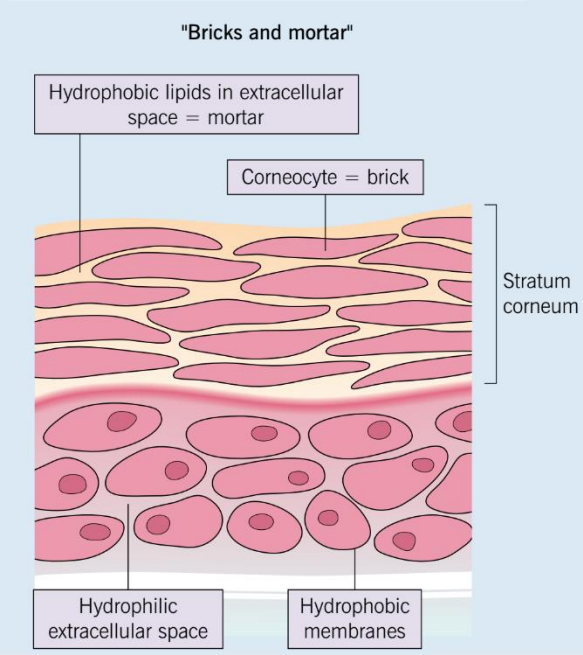

Fig. 2 – Two-compartment "bricks and mortar" system [3]

The process of continuous shedding of corneocytes from the skin surface is called desquamation.[5] It balances proliferating keratinocytes that form in the *stratum basale*. The cells migration through the epidermis to the surface takes approximately fourteen days.[2]

The interior of the corneocytes is filled with keratin filaments embedded in a matrix consisted principally of filaggrin (filament aggregating histidine-rich protein) and its breakdown products. These amino acids together with certain ions, such as chloride, sodium, lactate and urate, form the natural moisturizing factors (NMFs).[2] NMFs are endogenous humectants that keep the hydration of the *SC* on an adequate level. It is important for skin elasticity and permits regularly function for hydrolytic enzymes of desquamation.[15] Reduced levels of filaggrin and properly the Natural Moisturizing Factors (NMFs) are caused by mutations of the filaggrin gene connected with atopic dermatitis, ichthyosis vulgaris, psoriatic skin, ichthyosis, and general xerosis (dry skin).[4, 15]

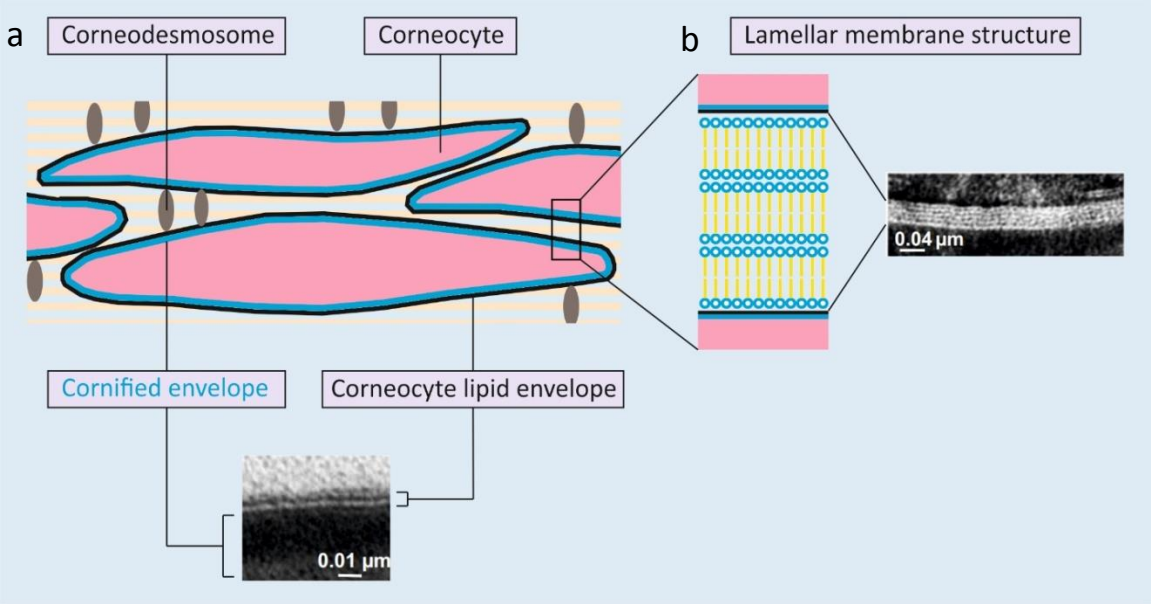

Fig. 3 – **a.** *Stratum corneum* structure: cornified envelope (blue); corneocyte lipid envelope (CLE, black); corneodesmosome (brown). **b.** Lamellar membrane structure with intercellular lipids. Insert, electron micrograph: Murine skin was fixed in Karnovsky's fixative, and post-fixed with 1 % aqueous osmium tetroxide, containing 1.5 % potassium ferrocyanide. Adapted from Uchida [4]

Corneocytes are enclosed by a cornified envelope (CE) that is formed by structural proteins crosslinked by transglutaminases.[3] CE has a stable stiff property to withstand mechanical barrier stress (Fig. 3a), and is surrounded by a layer of corneocyte lipid envelope (CLE).[4] This CLE is a support to form lamellar membrane structures and controls exit of hydrophilic agents from corneocytes, but the roles of CLE in the *SC* remain unidentified.[4]

The extracellular space in the *SC* is filled by lipid-enriched layers.[4] The lipids form lamellar membranes that stretch out in a horizontal direction parallel to the corneocytes (Fig. 3b). In addition, corneodesmosomes are found in the lamellar membrane structure. They are modified desmosomes including corneodesmosin, a structural protein that determines corneocyte adhesion.[2] Corneodesmosomes consist of desmoglein-1 and desmocollin-1 connected to other corneocytes, intensify cohesion and regulate desquamation by their pH-dependent degradation.[4]

1.1.2 *Stratum Corneum*: lipid composition

Composition of *SC* is generally 20% of lipid and 70% of insoluble keratins.[16] The majority of lipids is synthetized by keratinocytes in *stratum granulosum* and packed in lamellar bodies.

These organelles deliver their lipid content in the extracellular space by fusion with the plasma membrane of keratinocytes of the *stratum granulosum*.[8]

The *SC* lipid composition research began as early as 1959, when 'the chemical composition of human epidermal lipids' was published.[17] Development of methods such as gas/liquid chromatography (GLC) and nuclear magnetic resonance (NMR) studies improved the level of detail on this skin layer lipid composition.[18]

Finally, the main components of the extracellular matrix are ceramides, cholesterol and free fatty acids, which are present in approximately equimolar ratios.[3, 5, 19] Ceramides constitute approximately 50% of *SC* lipids mass [3, 5, 8] and have a critical role for the lamellar organization of this layer barrier.[3]

The 14 ceramides classes, embracing 342 individual ceramide forms, have been recognized in the human *SC.*[19] Of these, acylceramides or ceramides 1, 4 and 7 are epidermis-unique substances, which contain essential fatty acids in an ester linkage and important for barrier.[3, 5]

Each ceramide molecule contains a polar head group from sphingoid component (sphingosine, phytosphingosine, 6-hydroxysphingosine or dihydrosphingosine) (dotted circle on Fig. 4) and two hydrocarbon chains derived from a fatty acid, a sphingoid or fatty acid ester moiety.

Fig. 4 shows two molecular conformations of ceramides: the ‘hairpin’ or ‘tuning fork’ with the hydrocarbon chains pointing to the same direction and the extended or ‘splayed chain’ conformation, where the hydrocarbon chains adopt opposite directions.[5]

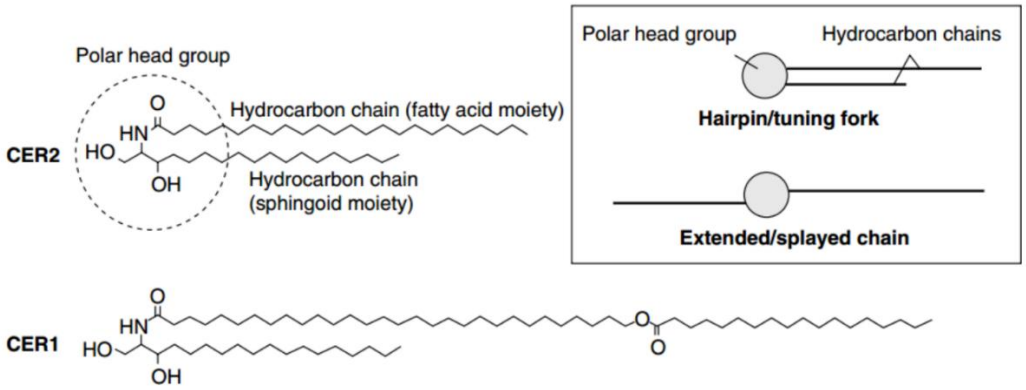

Fig. 4 – Chemical structures of two *SC* ceramides and their possible conformations [5]

The polar head groups can establish side hydrogen bonds and form lattice structures inside the lipid bilayers. In general, the hydrocarbon chains are saturated. The typical ceramide has a total of 38–54 carbon atoms.[4, 5]

Cholesterol is the second most prevalent lipid by weight in the *SC* (25%).[3, 8, 20] The increment of cholesterol concentration in the lipid bilayers correlates with the diminution of the membrane thickness and density, and at the same time with an extension of the membrane surface area. Cholesterol fluidizes the *SC* lipid bilayers at skin temperature.[5, 20]

Content of free fatty acids (FFAs) is 10 – 15% of the *SC* lipids. FFAs consist mainly of very-long-chain species with ≥18 carbon atom and are mostly saturated, like ceramides.

In addition to lipid species, cholesterol sulfate is typically at 2–5 % weight ratio. Its potential functions are to help in the formation of the lipid lamellae and stabilization of the *stratum corneum* by inhibiting enzymatic degradation of corneodesmosomes.[3, 5]

Any changes in the concentrations of these main lipid components can damage barrier integrity that mediates normal barrier function.

1.1.3 *Stratum corneum*: functions

Stratum corneum accomplishes barrier and immune functions. The most important properties of *SC* are presented in Table 1.

The epidermal permeability barrier prevents intake and uptake of compounds. The *SC* barrier functions may be partially connected to its low hydration of 15%–20% and its very high density (1.4 g/cm^3 in the dry state).[16] The body temperatures maintenance and water balance are regulated by blocking surplus evaporation of water from nucleated layers. One of the basic properties of this barrier is the prevention of penetration of allergens, microbial pathogens and xenotoxic chemicals.[4] As a general rule, a compound with molecular weight (Mw) larger than 500 Dalton cannot pass through the *SC*.[21]

The epidermis has a pH gradient: the extracellular pH stays neutral between the *stratum granulosum* and *SC*, where it becomes more acidic to ca. 4.5 at the outer *SC* layer (Fig. 1). Acidification enables antimicrobial activity and regulates, by enzymatic activity (proteases), the formation and desquamation of the epidermal barrier. The usage of alkaline or neutral soaps lead to the increase of the *SC* pH, which conducts to untimely cleavage of corneodesmosomes, decline in *SC* cohesion and following impairment of the epidermal barrier. The pH changes are

reported to matter in the pathogenesis of skin diseases such as atopic dermatitis, acne vulgaris and *Candida albicans* infections.[2] For example, with pH below 5.5, the growth of *Pseudomonas* acne, *Staphylococcus epidermidis*, and a virulent microbial pathogen, *Staphylococcus aureus*, are inhibited.[4]

Table 1 – Barrier roles of *SC* in maintaining epidermal homeostasis

Barrier	Roles	Effectors
Permeability	Prevents excess water loss	Primarily extracellular lamellar membrane structures
	Maintains body temperature	
	Prevents ingress of xenotoxic chemicals and allergens	
	Prevents invasion of microbes	
Antimicrobial	Protects against diverse microbes (Gram-positive and Gram-negative bacteria, fungi, and viruses)	Antimicrobial peptides
		Acidic pH
		Sphingoid bases
Antioxidant	Protects epidermis from oxidative stress	α-/γ-tocopherol
		Ascorbic acid
		Glutathione
Mechanical	Protects epidermis from mechanical stress	Primarily cornified envelopes
UV	Protects epidermis from cell death, DNA damage, and oxidative stress	Urocanic acid
		Structural components (proteins, lipid, nucleotides)

Adapted from Uchida.[4]

The permanent bacterial flora in the skin presents a comprehensive ecosystem. *Staphylococcus* and *Micrococcus* strains and Diphtheroid bacilli are the main part of nonpathogenic microflora. They consume the sebum like basic nutrient, restrain skin colonization by potentially pathogenic organisms that protect the skin against pathogenic one.[8]

SC plays also an important role in the innate immunity, which is related with the presence of antimicrobial peptides such as cathelicidin, dermcidin, RNase7, S100A7/psoriasin and defensins. They show potent antimicrobial activities against a wide spectrum of microbes, including gram-negative and gram-positive bacteria, fungi, and some viruses. Cathelicidin antimicrobial peptide (CAMP) is inducible with infection, injury or inflammatory response and stimulates the production of a signal lipid, sphingosine-1-phosphate (S1P) under stress conditions and activate vitamin D receptor (VDR). The defensins are classified in three subfamilies, α-, β-, and θ-defensin. They are inducible peptides in epidermis in response to microbial infection, inflammation, and differentiation.[4]

Adaptive immunity in the *SC* is associated with the availability of urocanic acid. The trans form of urocanic acid is generated from histidine (principally from NMF) by histidase, but can be converted to the cis form through exposure to ultraviolet (UV) radiation. Cis urocanic acid binds to the serotonin [5-hydroxytryptamine (5-HT)] receptor to eliminate immune function.[22] Urocanic acid is an epidermal major chromophore, which works as a powerful endogenic UV absorbent. Most lower UV wavelengths (UVB = 280–315 nm) are absorbed in the epidermis, but longer wavelengths (UVA = 315–340 nm) get to the dermis. Also the bulk amounts of proteins, lipids, and nucleotides have individually low potent chromophores, but together can form the UV barrier.[4]

The *SC* is constantly exposed to oxidants, including UV light, chemical oxidants and air pollutants. α- and γ-Tocopherol, ascorbic acid, and glutathione are the chief hydrophobic anti-oxidants of *SC*, providing the lipid bilayers stability and safeguarding from lipid peroxidation.[8]

1.1.4 Viable Epidermis

The part of the epidermis that is formed by many layers of closely packed nucleated cells, with the exception of the *SC*, is called as the viable epidermis.[5] The epidermis has an undulated geometry and connects with the dermis (Fig. 1) partially by fitting together projections (epidermal ridges or pegs) and recesses (dermal papillae).[1]

The viable epidermis is generally 50–100 μm thick and contains no blood vessels and sensory nerve endings.[3, 5] It is mainly constituted by keratinocytes (approximately 95% of cells), but three other types of cell are also found there: melanocytes, Langerhans cells and Merkel cells.[5, 23] Keratinocytes originate from the stratum basale and expose oneself to progressive differentiation while migrating to the *SC* (described earlier, see Section 1.1.1) they are

necessary to maintain the *SC* by replacing lost corneocytes and *SC* lipids during desquamation.[5] The steroid 7-dehydrocholesterol, present in keratinocytes, is transformed by sunlight to cholecalciferol. Activation of vitamin D takes place in the kidney.[1] The viable epidermis is considerably hydrophilic (> 50%) in the opposite to *SC*.[24]

1.1.5 Dermis

The dermis is typically 1–2 mm thick and consists of collagenous (70%) and elastin fibers which give elasticity, flexibility and strength to the skin.[3, 5] Hair follicles, sebaceous glands, sensory nerve endings, sweat glands, lymphatic vessels and blood capillaries found in the dermis and extend the dermal-epidermal junction. It allows to provide nutrients and oxygen delivery for both the dermis and epidermis.[23] The dermis contains a range of immune cells including macrophages and dermal dendritic cells. It interplays with keratinocytes to provide stability of skin structure and heal over damage. The thermal barrier, energy depositary and protection from physical stroke is mainly connected with adipose tissue associated with collagen fibers, found in the lower reticular dermis layer. The water content in the dermis reaches 70%, promoting absorption of hydrophilic drugs.

1.1.6 Hypodermis

The subcutaneous layer or hypodermis is the innermost layer of the skin and consists of fat cells. However, this layer can be absent in some thin skin, for example on the eyelid. The hypodermis is between the skin and the subjacent tissues of the body, such as muscles and bone. Larger lymphatic and blood vessels are standing in this layer. Consequently, the major functions of the hypodermis are insulation, mechanical integrity and support and conductance of the vascular and neural signals of the skin.[5, 23]

2 Skin penetration

The skin is an attractive site for drug delivery and cosmetics. But normal skin is a serious barrier to drug absorption, which is why pharmacologists and cosmetologists became interested in the development of new drugs and ways of delivery (Table 2). Comprehension of the factors that influence the permeation via this barrier is necessary to obtain an effective transdermal therapy.[3, 8]

Table 2 – Physical, chemical, and biological factors modulating the rate of penetration

Physical and chemical factors	Biological factors
Molecular mass	Age
Concentration	Condition of the skin
Solubility	Metabolism of the skin
Partition coefficient	Hydration of the skin
Variations of pH	Compound–skin interactions
Co-solvents	
Temperature	
Penetration enhancers	

Adapted from Pouillot. [8]

Physical, chemical, and biological factors have an impact on the cutaneous absorption. They include molecular weight (preferentially lower than 500Da) [21], concentration, solubility, octanol/ water partition coefficient (very lipophilic molecules will distribute in *SC* but will transit with problems and hydrophilic molecules have bad intrusion), pH variations, co-solvents (increment the mobility of molecules), temperature (heat increases penetration), and penetration enhancers.[8]

The biological parameters that influence the rate of skin penetration are age, skin type, level of the hydration, thickness of *SC*, amount and size of hair follicles or sweat ducts, condition, metabolism and sex hormones. Thus, skin location on the body has an important role in drug therapy.[8]

2.1 Routes of drug penetration through the skin

There are four possible routes of drug penetration across the intact skin (Fig. 5): intercellular, intrafollicular, transcellular and polar.[8] Sometimes, the diffusion through the skin appendages (hair follicles and sweat glands) combine into the appendageal route.[5, 25] Besides, the intercellular and transcellular ways are named the transepidermal pathway. The integrated flux of these all pathways defines the general observable flux through the skin.[5]

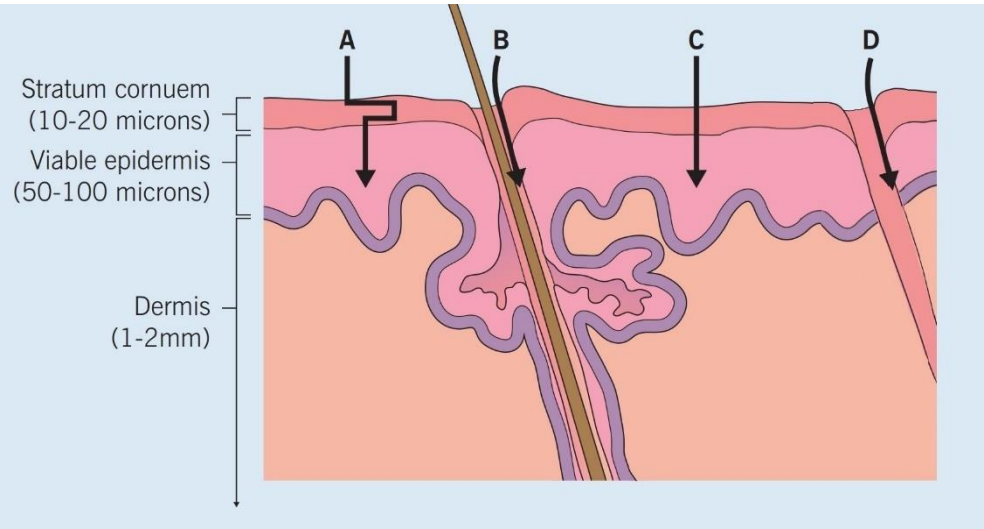

Fig. 5 – Pathways into the skin for transdermal drug delivery. **A.** Intercellular pathway (penetration between the corneocytes through the intercellular lipids). **B.** Intrafollicular pathway (penetration through the hair follicles). **C.** Transcellular pathway (penetration through the corneocytes). **D.** Polar pathway (penetration through the polar pores) Adapted from Prausnitz [3]

2.1.1 Intercellular pathway

Transport through the intercellular area provides diffusion of lipophilic or non-polar compounds via the continuous lipid matrix.[23] Furthermore, cationic molecules have a more effective adhesion with the negatively charged *SC*.[8] In this pathway, the penetration goes by the tortuous path inside of the extracellular lipids and not cross the *SC* corneocytes. These lipids account for approximately 20% of the total volume of *SC*, but are the major way of penetration for most compounds. The matrix is separated in two parts: a nonpermeable area (gel) and a permeable area (liquid-crystalline). The widest intervals between the intercellular lipids are 0.013 μm. About 90% of the molecules penetrate the skin by this pathways due to lamellar organization of lipids.[8] The lipid-enriched matrix of the *SC* not only limits transdermal delivery of hydrophilic drugs, but it works like *SC* "reservoir"– for the lipid-soluble drugs, which can amass and be slowly released, as for example topical corticosteroids.[3] The majority of skin permeation enhancers, such as dimethylsulphoxide (DMSO), glycols and surfactants, can react with intercellular lipid bilayers by decreasing its diffusional resistance.[3, 8]

2.1.2 Transcellular pathway

The transcellular pathway via corneocytes, which abounds in keratin, allows the transport of hydrophilic or polar substances.[23] It needs crossing the interlaced layers of cells and

extracellular matrix. Numerous stages of partition and diffusion are required to penetrate the drug through the cell matrix. The electrical (electroporation/ iontophoresis), mechanical (sonoporation/ sonophoresis) or thermal stimulus can give the gain of transdermal drug transport.[9]

2.1.3 Appendageal pathway

The skin appendages are hair follicles and sweat glands, which have a role in heat regulation and elimination of acids and body wastes. Its length is about 2-5 mm, from *SC* to dermis or hypodermis. Various sweat glands, oil glands, hair follicles and pores opening to the outer surface of the skin via their ducts, that can be used like possible way for entry. The nature of the pathway, arising in the sweat glands, is hydrophilic. These polar pores are located between cells and encircled by polar lipids, which make small holes in *SC*. The follicular orifices occupy only 1–2% of the total skin surface area and use for the intrafollicular way, sometimes in mixture with different surfactants and glycols.[8] Hence, it was considered an inessential pathway for drug penetration. But current research found that hair follicles and sweat glands may offer an alternate pathway for a diffusing molecule.[9]

3 Transdermal drug delivery

Transdermal drug delivery (TDD) is a pain-free way of delivering drugs by applying a drug formulation onto the skin. The medicine firstly passes through the *SC* and then permeates via the viable epidermis and dermis by diffusion. After reaching the dermal layer, the drug becomes available for the uptake into the systemic circulation.[23]

TDD has some advantages and disadvantages over other traditional routes of drug delivery (Table 3). The dermal and transdermal delivery systems have a lot of advantages in comparison with the oral route and hypodermic injections, but also have the limitations listed on Table 3. Nevertheless, TDD takes an important role in drug delivery and stays a demanding process notwithstanding the ability for potential skin absorption.[9]

Table 3 – Transdermal drug delivery: theoretical benefits and limitations

Benefits	Limitations
▪ Painless self-administration for patients. ▪ Improved efficacy, i.e. continuous release. ▪ Reduced toxicity: no “peaks” and lower total absorbed dose. ▪ In case of toxicity, the transdermal patch can easily be removed by the patient. ▪ Avoidance of hepatic first-pass metabolism and the gastrointestinal tract for poorly bioavailable drugs. ▪ Decreased dosing frequency ▪ Decreased costs to patient due to decreased: total dose and dosing frequency (increased efficiency), as patches are designed to deliver drugs from 1 to 7 days. ▪ Multiple dosing, on-demand or variable-rate delivery of drugs is possible with the latest programmable systems.	▪ Not all drugs are suitable for transdermal delivery. Drug requirements for TDD are high permeability, $\log P_{o/w}$=2-3, Mw < 500 Da, dose less than 10 mg. ▪ Drugs that require high blood levels cannot be administered. ▪ The adhesive used may not adhere well to all types of skin. ▪ Drugs or drug formulation may cause sensitization or irritation which must be evaluated early in the development process. ▪ The patches may/can be uncom-fortable to wear. ▪ Specialized equipment for production, which results in more expensive medicines. ▪ Not suitable for drugs requiring rapid onset of action (TDD has a lag time).

Adapted from Prausnitz and Uchechi. [3, 9]

3.1 Skin models

Validated data about permeation of compounds through human skin are needed for pharmaceutical, cosmetic and toxicological purposes. An efficient method for development and rationalization of drug formulation for the skin, demands specific skin models capable of estimating and determining topical properties of the formulation. After the identification of

important penetration and permeation properties (wanted and unwanted) for the drug formulations, its optimization becomes achievable.[10]

3.1.1 *Ex vivo* models

During long time, the main way for the preclinical research of new drugs and for the optimization of topical drug formulations was the exploitation of *ex vivo* models.

Human skin is absolutely the most suitable model for study TDD.[26] Skin obtained from different origins: plastic surgery, amputation and cadaver, have been applied to *ex vivo* permeation assays. Generally, the skin samples can be collected from the abdomen, back, leg or breast.[27] However, the use of human skin is very limited by the ethical permissions, regulatory issues and laboratory facilities. The European Union prohibits to get financial benefit from the utilization of human tissue, that is why widely-distributed usage is impossible.[28] Besides, the skin permeability is very changeable between the samples obtained from equal or different anatomical places of the same donor and has unpredictable character with different subjects or different age groups.[10]

The *ex vivo* pig skin models are the most relevant animal models because of the multiple anatomical, physiological and histological resemblances to human skin such as the dermal/ epidermal thickness ratio, epidermal thickness, similarity in hair follicle and blood vessel density in the skin and content of *SC* ceramides, dermal collagen and elastin.[29] The pig skin is easily obtained as a waste from animals slaughtered for food. The central outside part of the porcine ear has been recommended because of the analogy with human skin layers. Variability of permeability in different samples of pork skin also takes place. The pig ear skin permeability is comparable with human skin. In fact, studies showed a good correlation especially for lipophilic substances.[10]

A wide spectrum of animal models involves the primates, mouse, rat, guinea pig, rabbit, bovine (udder) and snake (slough – shed skin) models. However, the primate research is highly restricted and very expensive. All these models besides bovine requires ethical permission in opposite to pig skin models. The dissimilarities in the thickness of SC, hair density, number of corneocyte layers, hydration, lipid profile and morphology are reasons of advantages and limitations and are listed on Table 4.[10]

Since 2009, the use of animals for collection of toxicological data for cosmetic ingredients has been prohibited in the EU (76/768/EEC, February 2003).[28] That led to an expressed interest in *in vitro* models, which allow the penetration, permeation and skin irritancy assays.

3.1.2 *In vitro* models

The using of skin equivalents started from normal human keratinocytes (NHKs) as a model for skin irritancy. There are several methods for growing keratinocytes. The culture of NHKs begins with a small piece of human skin (about 0.5-1 cm^2) obtained from surgery after separation and specific treatment, that grows easily in culture medium. It allows the use of a large number of cells, leading to the opportunity for wide-ranging toxicity screening tests with many substances in a broad concentration range. This model has no *SC* layer, shows good ability for testing of water soluble compounds and less capability for evaluation of poorly soluble compounds and complex formulations.[30]

The model has improved with its application in membranes, which support the NHKs during growing and forming the reconstructed human epidermis. The commercially obtainable models of the human epidermis (EpiSkin®, EpiDerm®, SkinEthic®) or full thickness skin (Phenion®) apply this approach in practice.[28, 31] More improved models are the full-thickness skin consisting of the fibroblast populated collagen matrices (dermis equivalent) and an epidermal cover representing NHKs.[28] They are well confirmed in a large German study.[32] The results point to a higher permeation of the reconstructed skin models than of human epidermis and pig skin. Nevertheless, they are relevant alternatives for the *in vitro* rating of the permeation and penetration of substances when applied as aqueous solutions, especially in the early phases of drug formulation development.[32]

To facilitate the determination of skin permeability, a few *in vitro* models have been presented, for example the silicone membranes or poly(dimethylsiloxane) (PDMS) [33], PAMPA (the ceramide-derived parallel artificial membrane permeability assay) [34] and the phospholipid vesicle-based permeation assay (PVPA).[35]

The first PAMPA system included an artificial membrane from hydrophobic filter coated with phosphatidylcholine as a membrane barrier, which differentiates the donor and acceptor parts. That model was oriented for testing the transcellular intestinal permeability. Sinko *at al*. designed the skin-PAMPA, which consist of ceramides analogues called the synthetic ceramides, as substitution for native ceramides found in *SC*. The skin-PAMPA was used in the skin permeability studies.[34] The disadvantages are shown on Table 4.

Table 4 – Characteristic of different skin models used for optimization of topical formulation

Skin model	Advantages	Limitations
Silicone model membranes	Reproducible Low cost Storage	Non-lipid based Low resemblance to SC Non-biological origin
PAMPA	Reproducible Prolonged storage capabilities Low cost	Synthetic lipids/non-lipid based Lipid organization not characterized Low resemblance to SC Non-biological origin
PVPA	Reproducible Lipid composition easily modified Relatively low cost Storage	Lipid organization not characterized Non-biological origin
Stratum corneum substitute	Mimicking *SC* lipid organization Steady state flux similar to human *SC* Reproducible Lipid composition easily modified Relatively low cost	Not used in formulation optimization yet Non-biological origin
Reconstructed human skin equivalents	Consistence in permeability in comparison to human skin	More permeable than human skin Questionable barrier function High cost
Pig ear	Easily obtained (waste from slaughter) Similarity with human skin	Age of animal influences skin thickness Removal of hairs (skin damage) Storage
Newborn pig	Thickness of the *SC* is similar to human horny layer	Higher number of hairs than in humans Different anatomical sites: abdomen, back Difference in the skin thickness; newborn and older animals Storage
Mouse	Small size, uncomplicated handling Hairless species available	Ethical permission Very thin skin, highly permeable High density of hair follicles Removal of hairs (skin damage)

Rat	Small size, uncomplicated handling Hairless species available	Ethical permission Thin skin, more permeable than human High density of hair follicles Removal of hairs (skin damage)
Guinea pig	Similar permeability to human and pig ear skin Hairless species available	Ethical permission High density of hair follicles Removal of (skin damage)
Rabbit	Ears as waste from slaughter Similar permeability to guinea pig	Ethical permission High density of hair follicles Removal of hairs (skin damage)
Shed snake	Single animal provides repeated sheds Multiple samples from one shed Storage at room temperature	Absence of hair follicles Differences in skin metabolism, compared to human skin Absence of living epidermis and dermis
Bovine udders Perfused bovine udder skin (BUS)	Easily obtained (waste from slaughter) BUS-comparable to living skin Multiple samples from one animal	One donor enables testing of only one sample (BUS) Weaker barrier to some drugs than pig skin Storage
Human	The most relevant model	Ethical permission Higher inter- and intra-variability than with porcine ear skin Different sources: age, sex, race, plastic surgery, amputation, cadaver Different anatomical parts: abdomen, tight, breast, back, etc. Storage

3.2 PVPA model

Lately a new PVPA model, which imitates the *SC* barrier of the skin was developed.[35] Although the original PVPA was presented as model for screening the intestinal permeability and is composed of a consistent coat of liposomes deposited on a filter support acting as biological barrier (Fig. 6).[6, 36]

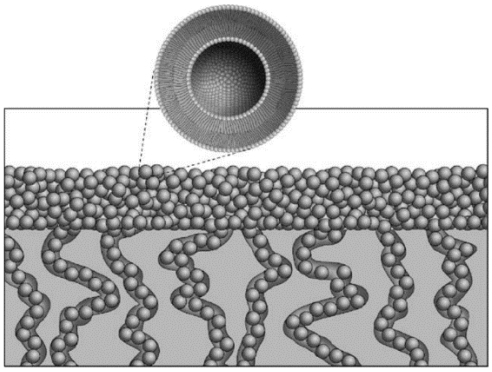

Fig. 6 – A schematic representation of the estimated layout of PVPA [6]

The arrangement shown in Fig. 6 is based on hypothesis and implies that the liposomes are located within the pores and on the surface of the membranes.[6] The PVPA barrier has good abilities for a high-throughput permeability screening model [37] and is easily changeable in the composition of the liposomes making possible to mimic various absorption barriers. The PVPA can mimic different biological barriers just by the change of the lipid constituents in the models.[35] In resume, skin PVPA models have been prepared with two different lipid compositions:

- PVPAc consists of liposomes made of cholesterol (22.9%, w/w) and egg phosphatidylcholine EPC (77.1%, w/w).[35]

- PVPAs from lipid mixture (EPC (50%, w/w), ceramide (27.5%, w/w), cholesterol (12.5%, w/w), free fatty acid (7.5%, w/w) and cholesteryl sulfate (2.5%, w/w).[35]

The permeability of compounds was evaluated in these PVPA skin models. The results were compared with reported permeabilities using animal skin (rat, cattle, dog and pig) and estimated *in silico* values. The PVPA permeability data mainly corresponded with the literature values of the animal skin penetration assays and the calculated values with the exception of flufenamic acid that showed a relatively lower permeation.[35]

In a following study, the PVPAs model was examined with different types of liposomes containing diclofenac sodium salt. The results showed a rising permeation ranking of diclofenac sodium from liposomal formulations correlating with the physicochemical parameters of the liposomal vehicle. The permeability of diclofenac increased in the availability of the penetration enhancers and edge activators within the liposomes.[38]

Recently, the developed PVPA skin models were compared with the reconstructed human skin model, EpiSkin®. The permeability result indicates that the PVPA has the ability to differentiate between the liposomal formulations and drug solutions as opposed to EpiSkin®. In short, the PVPA models were better than EpiSkin® concerning their potential to determinate the influence of the formulations on the drug permeability which could be used in drug development at early stage. Moreover, PVPA barriers had straightforward, effectiveness, economical and long storable.[39]

4 Aims and Strategy

The ability of skin models to predict permeation of trans(dermal) drug formulations has high significance for both drug therapy and cosmetic treatment.[38] In the current time, prohibitions and limitations regarding animal skin usage lead to an increasing interest in the investigation and development of *in vitro* models. The PVPA model is one of them, and has showed good results and wide perspectives for the early design stages of drugs and cosmeceuticals.[35, 39]

The aim of this study was to develop phospholipid vesicles models with adequate composition to reproduce the *SC* most accurately. Two objectives were identified for this study: 1) to design and characterize phospholipid-based permeation assay membranes; 2) to compare permeabilities obtained with the *SC* model and in animal skin.

II MATERIALS AND METHODS

1 Materials

Stearic acid was obtained from Merck KGaA, Darmstadt, Germany. Egg chicken ceramide, cholesterol (ovine wool) were purchased from Avanti Polar Lipids (Alabaster, Alabama). L-α-Phosphatidylcholine (egg yolk), calcein, Dulbecco's phosphate buffered saline (PBS), sodium cholesteryl sulfate, dimethyl sulfoxide, oleic acid, cremophor® EL (Kolliphor® EL), naproxen sodium, diclofenac sodium, cyclosporine, caffeine, sodium chloride, 2-[4-(2-hydroxyethyl)piperazin-1-yl]ethanesulfonic acid hemisodium salt (HEPES), potassium phosphate monobasic, L-ascorbic acid and perchloric acid were supplied by Sigma-Aldrich (St Louis, MO, USA). Methotrexate was a gift from Excella (Feucht, Germany). Ammonium molybdate was obtained from AnalaR® (BDH Laboratory Supplies, Poole, England).

96-well, black plate, flat bottom with lid and 24-well plate flat bottom with lid were obtained from Falcon, Corning Incorporated, NY, USA. 96-well UV-Star® microplate, flat bottom (Chimney well), µClear® were supplied by Greiner Bio-one, Frickenhausen, Germany. Millicell culture plate inserts, polycarbonate (tissue culture-treated, Isopore track-etched PVP-free polycarbonate, pore size is 0.4 µm, d = 12 mm) were purchased from Millipore Corporation, Merck KGaA, Darmstadt, Germany).

Double-deionized water was provided by an ultra-pure water system (Arium Pro, Sartorius AG, Gottingen, Germany). The reagents were weighted in a digital analytical balance Kern ACJ/ACS 80-4 (Kern & Sohn; Balingen, Germany). pH measurements were achieved using a Crison pH meter GLP 22 with a Crison 52-02 tip (Crison; Barcelona, Spain).

Pig ear skin was purchased from a local commercial butcher (Porto, Portugal).

2 Methods

2.1 Choice lipid composition for liposomes

To establish the conditions needed to the phospholipid vesicular model mimic only the human *SC* barrier [35, 38], a search of the *SC* lipid composition was conducted. The main components of the human *SC* lipid matrix, described in the literature, are ceramides (50% w/w), cholesterol (25% w/w), free fatty acids (10–15% w/w) and cholesterol sulfate (2–5 % w/w).[3, 5, 8] Thus, the following composition: ceramide (50% w/w), egg L-α-phosphatidylcholine (EPC, 25% w/w), cholesterol (12.5% w/w), free fatty acids (10% w/w) and cholesteryl sulfate (2.5% w/w) was selected to prepare the lipid-based vesicles. The relation between the commonly described as human *SC* lipid composition and the one selected for this work is showed in Fig. 7.

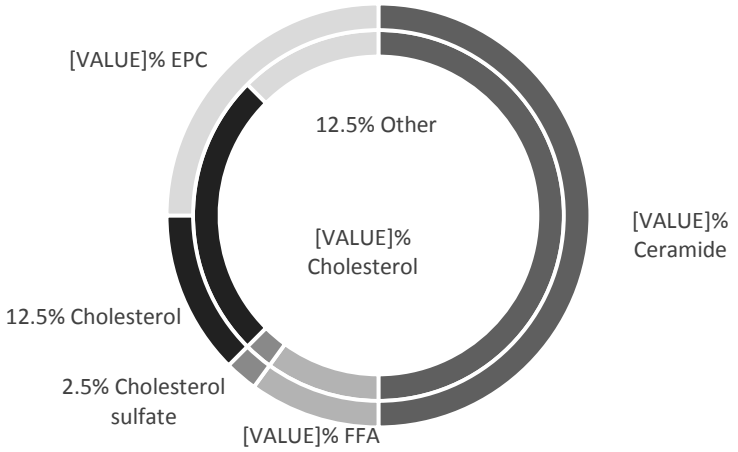

Fig. 7 – The comparison between an original lipid composition of *SC* (inside circle) and the composition, which is used in this study (outside part)

The addition of EPC is to assure the formation and longer stability of the liposomes [40] and a reduction in the cost of the model. Differences between lipid composition in previous literature works [35, 39] and this study consist in the attempt to have a more closely human *SC* lipid composition (here, about 86% lipids correspond to the *SC* layer).

2.2 Preparation of liposomes

The liposomes were prepared through the thin-film hydration method followed by sonication.[41] This method includes preparation of a thin lipid film in a round-bottom flask by the evaporation of organic solvents. Heterogeneous liposomes were formed by the addition and agitation of phosphate buffer (PBS), the multilamellar large liposomes (MLVs). Finally, after sonication large unilamellar liposomes (LUVs) were obtained.

2.2.1 Preparation of the thin film

Lipid mixtures were prepared according to Table 5 as a close approximation to the composition of human *SC* [42] but without the small proportions of cholesteryl esters and other minor constituents.

Table 5 – Liposomes composition

Component	Mass (%)	Mass (mg)
Ceramide	50	10.0
EPC	25	5.0
Cholesterol	12.5	2.5
FFA (Stearic acid)	10	2.0
Cholesteryl Sulfate	2.5	0.5
Total	100	20.0

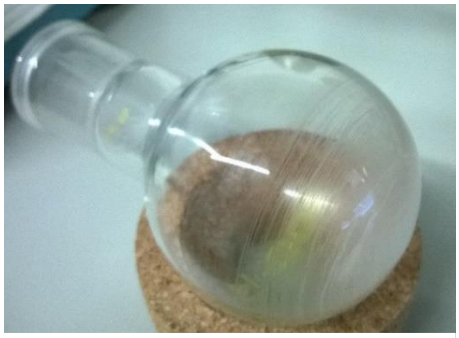

Fig. 8 – Thin-lipid film formation

The lipid mixtures (20.0 mg) were dissolved in a mixture of chloroform and methanol (3:2 v/v) and were transferred into a 100-mL glass round-bottom flask. The solvents were evaporated in a rotary evaporator under a nitrogen stream (P=1.0 Bar) and a heating bath at 40°C for 30 min (Fig. 8).

2.2.2 Hydration of the thin film

5 mL of PBS were added in the dry lipid film and vortexed 10 min at room temperature. A final concentration of 4 mg/mL (20 mg in 5 mL PBS) was obtained. Then repeated cycles of heating and vortex were performed until the lipid film was detached (Table 6). At the end all the lipid material was suspended in solution, the flask was covered with a piece of stretched parafilm to prevent the entry of dusts or contaminants and were left at 4°C overnight to assure an efficient hydration of the lipid materials. The next day, two cycles of heating/vortex were reiterated again for formation of multilamellar vesicles (MLVs).

Table 6 – Cycles of heating/vortex for liposomes preparation

Temperature	Heating time	Repeat
50°C	5 min	two times
60°C	5 min	two times
65°C	3 min	one-time
4°C	Store overnight	
65°C	5 min	one-time
70°C	5 min	one-time

2.2.3 Sonication

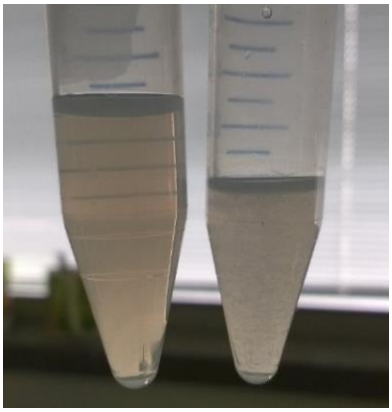

Fig. 9 – Liposome suspensions: LUVs (right) and MLVs (left)

The suspension of MLVs was divided into two portions to obtain liposomes of two different sizes. The ultrasonicator (Ultrasonic Processor for Small Volume Applications, Sonic Vibra-Cell) was used for LUVs production with amplitude 70% until the suspensions became clear (2 to 3 min) (see Fig. 9).[25] A schematic representation for this method is shown on Fig. 10.

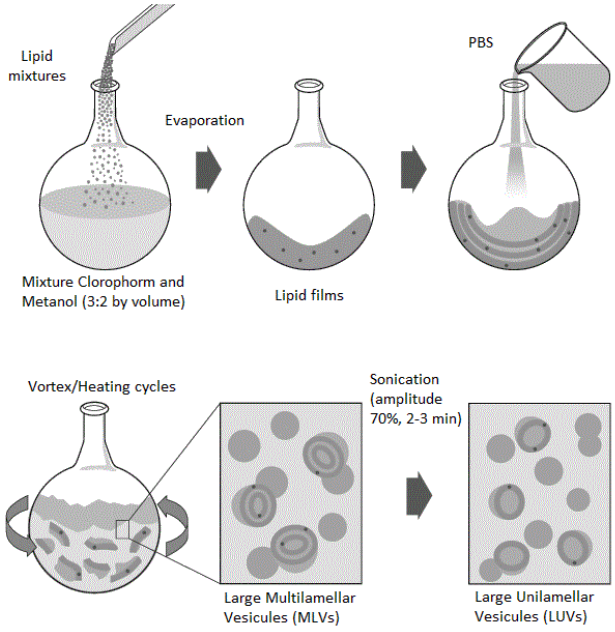

Fig. 10 – Schematic representation of liposomes preparation

2.3 Particle size and polydispersity index

Dynamic light scattering (DLS) is a well-known method for the characterization of particles, molecules or emulsions, which have been dispersed in a liquid. In DLS, the laser light is dispersed with various intensities depending on the Brownian motion of particles or molecules in suspension. Analysis of these intensity variations determines the velocity of the Brownian motion and therefore the particle size using the Stokes-Einstein equation.[43]

The mean size and polydispersity index (PDI) of the liposomes (LUVs and MLVs) were evaluated using a Particle Size Analyzer (Brookhaven Instruments Corporation; Software: Particle Sizing v.5 Brookhaven Instruments; Holtsville, NY, USA). The samples were diluted 20 x with PBS buffer and then analyzed under the following parameters: run – 2 times, run duration – 1 min, temperature – 25.0°C, angle – 90.00º, wavelength – 660.0 nm.

2.4 Preparation of the human *SC* model

The method involved the deposition of liposomes onto a filter support based of culture inserts, to obtain a barrier for transport studies. Phospholipid vesicle-based barriers were prepared as described previously, with few modifications.[35, 36] Briefly, the preparation of the human *SC* model is outlined in Fig. 11. Sterile culture inserts (pore size 0.4 µm, d = 12 mm) were used (Table 7). Freshly prepared LUVs and MLVs were vortexed and kept at room temperature before addition.

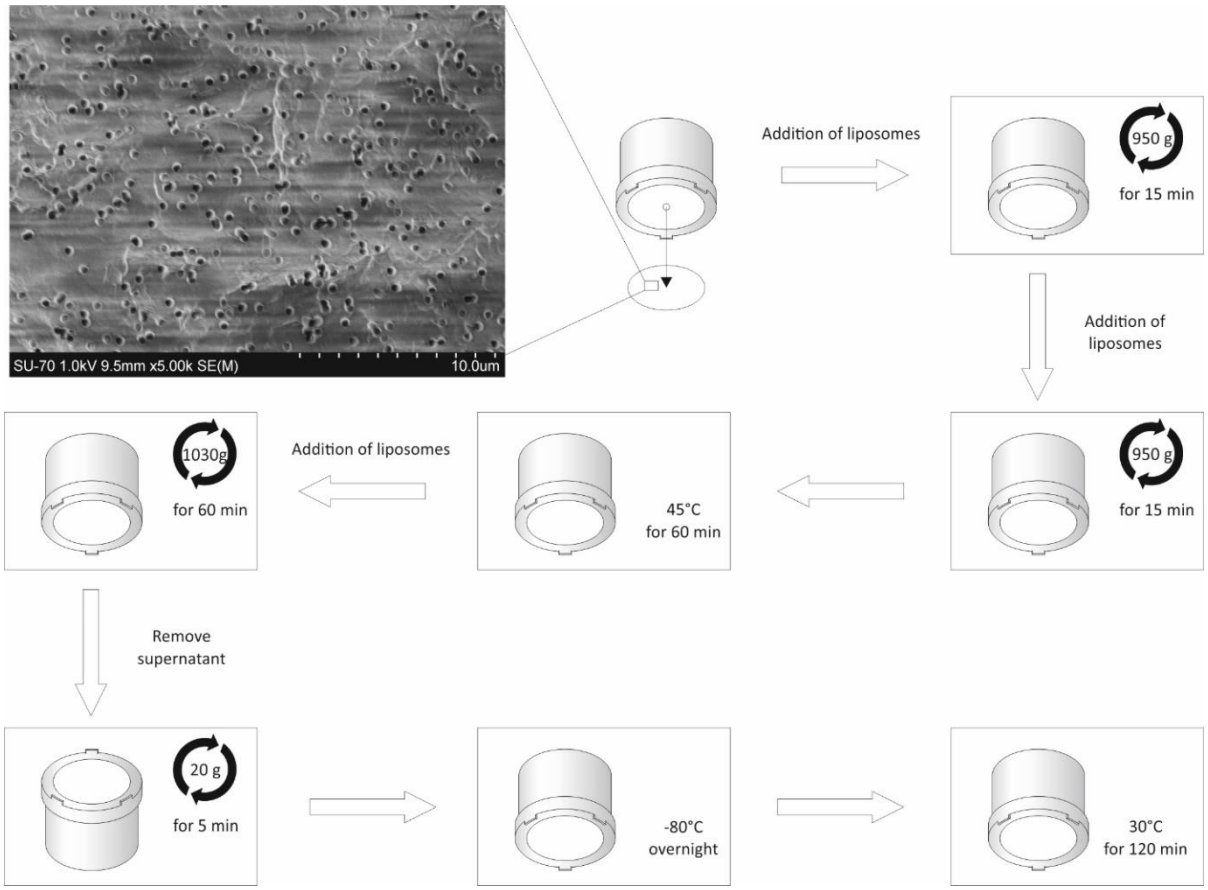

Fig. 11 – Flow chart for the preparation of the vesicular phospholipid barriers

In resume:

- An aliquot of liposomal suspension (100 µL of LUVs) was added to each culture inserts. The inserts were fixed into tubes, covered with a lid and centrifuged (Allegra X-15R, Beckman Coulter) at 950 *g* for 15 min at 20°C, to force the suspension pass through the filter.

- Then an additional amount of LUVs suspension (100 µL) was applied. The inserts were rotated 180° horizontally, followed by centrifugation under same conditions for 15 min.
- Thereafter, inserts were in open tubes and heated at 45°C for 60 min (new step in relation to the described protocol:[35] lower temperature and extended exposition of time because the inserts have temperature limit 50°C). This stage was made to enhance the viscosity of the suspension and to promote covering of the filter with liposomes.
- After another portion of the liposome suspension which contains MLVs (bigger liposomes) was added in the amount of 100 µL to each insert and centrifuged at 1030 *g* for 60 min at 20°C.
- Upon centrifugation, the excess of the supernatant was removed with a micropipette, the barriers were tilted at 45 degrees and the supernatant was accurately collected without touching the filter surface.
- Then, the inserts were centrifuged in an inverted position (Fig. 11) at 20 *g* for 5 min at 20°C.
- Thereafter, inserts were transferred to fresh dry wells in a 24-well culture plate, covered with a lid, and then were frozen at -80°C overnight and thawed in open wells at 30°C for 120 min in the next morning.

Table 7 – Specifications of the culture plate inserts

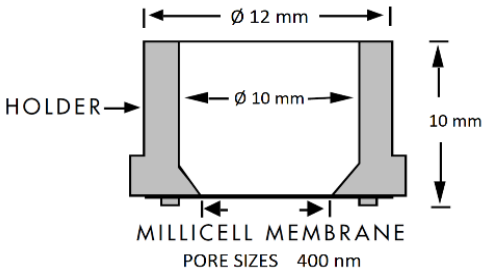

Height (including feet)	10 mm
Height of feet	1-2 mm
Outer Diameter	12 mm
Inner Diameter	10 mm
Membrane Area (effective)	0.6 cm^2
Temperature limit	50°C
Membrane pore sizes	0.4 µm

2.5 Test compounds

2.5.1 Calcein

Calcein (other name is fluorexon), is a widely known fluorescence dye.[44] It is a hydrophilic and charged marker exploited in the capacity of being an efficient indicator to describe the properties of (model) biomembranes [45] and to evaluate the trans-bilayer permeability.[46] Moreover the calcein-release effect has been explored with respect to the design of novel drug-

delivery systems [47] and calcein has been used like a model of hydrophilic and relatively low molecular weight (622.55 g/mol) drug.[48] Calcein has been also used as a reference compound and an indicator of potential aqueous pathways in the lipid layer due to its chemical properties.[49] Thus, to confirm the model's ability to evaluate skin drug permeation a solution of calcein was applied.[50]

The stock solution with 1 mM concentration was prepared by dissolving calcein in buffer pH 7.4 (PBS or HEPES for phospholipid quantification assay) on a sonication bath (Sonica® Ultrasonic Cleaner). It was stored at room temperature and protected from light sources. The different standard solutions (1.56 - 25 $\cdot 10^{-3}$ mM) were prepared and the fluorescence measured in a microplate reader (Synergy™ HT Multi-Detection Microplate Reader, BioTek®) with excitation and emission wavelengths at 485 nm and 528 nm, respectively, for the linear calibration curve.

2.5.2 Drugs

The drugs: caffeine, naproxen, diclofenac, methotrexate and cyclosporine were chosen to validate the *SC* model. They cover a wide range of physicochemical properties (molecular weight, pKa, log D and polar surface area, PSA), which are shown in the Table 8.

Table 8 – Physicochemical properties of the drugs used in this work

Drug	Mw	log D[a]	PSA[a]	pK_a[b]	F_a (%)[a]
Caffeine	194.2	0.02	59.2	14 (25°C)*	100
Naproxen sodium	252.24	0.23	56.2	4.15	98
Diclofenac sodium	318.13	1.15	42.4	4.0	100
Methotrexate	454.44	−2.53	225.9	4.7	47
Cyclosporine	1202.64	2.31	-	9.45*	35

[a] Log D (partition coefficient), PSA (polar surface area) and F_a (fraction absorbed in humans after oral administration) values were taken from Zhu.[51]

[b] pK_a (dissociation constant) values were obtained from Prankerd [52] except those which marked with * which were taken from Swarbrick, Luo [53, 54] and Oliyai.[55]

Caffeine is a stimulant of the central nervous system and may evoke sleepless and promote mental ability.[56] The main benefits asserted for application of caffeine in cosmetics lies in averting redundant fat accumulation in the skin, lymphatic drainage promotion and skin

protection against the UV radiation. Scientific proof for many of these described advantages is missing and most of the literature studies are based on cell culture or mouse models.[57] Nevertheless, caffeine is recommended as a test substance by the OECD (Organization for Economic Co-operation and Development) because it has been extensively studied *in vitro* and *in vivo*.[58] Also it is used as a model hydrophilic compound in dermal risk assessment studies and skin toxicology.[54]

Naproxen and diclofenac are two non-steroidal anti-inflammatory drugs (NSAIDs) and they are generally prescribed for patients affected by dermatitis [59] and rheumatic diseases.[60, 61] Lately, development of various strategies such as penetration enhancers and the prodrug approach has been utilized to enhance the topical absorption of NSAIDs.[62, 63]

The chemical formulas and structures of the studied drugs are presented in Fig. 12.

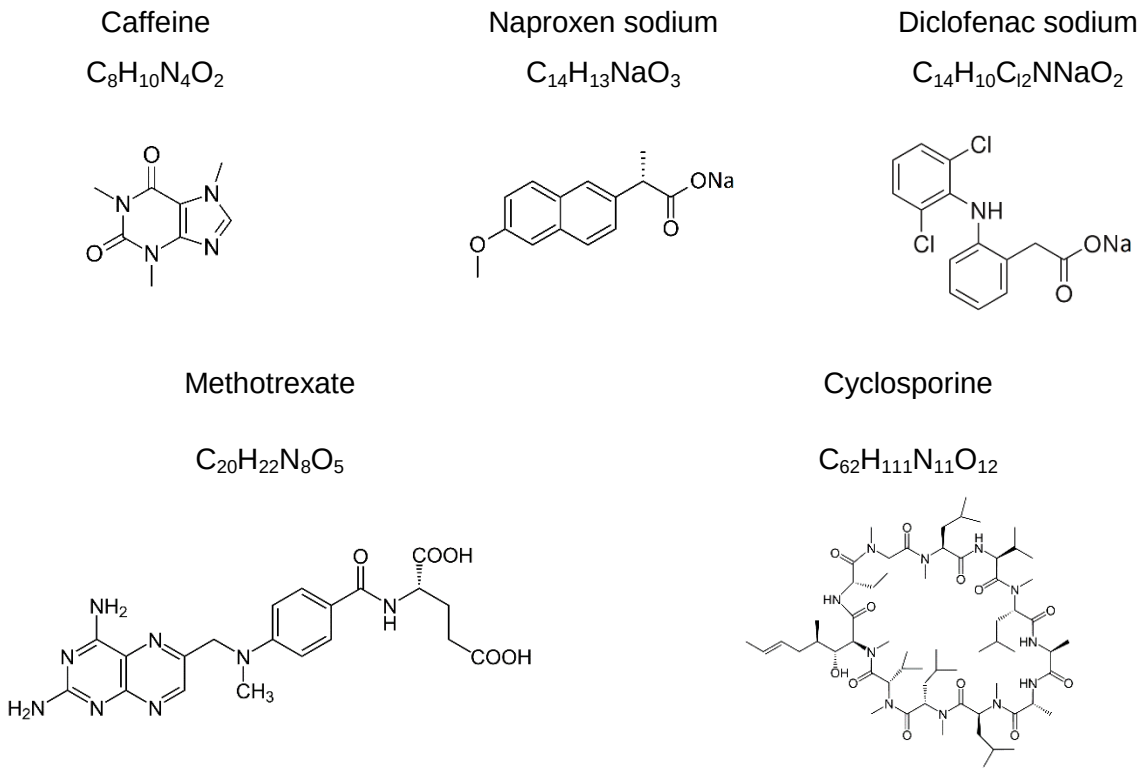

Fig. 12 – The chemical formulas and structures of the studied drugs

Methotrexate is an antimetabolite drug, which has anti-inflammatory and immunosuppressant properties. It has shown effective abilities in treating diseases such as

tumors (e.g. skin and breast cancer, osteosarcoma), psoriasis and rheumatoid arthritis.[64] However, one of the methotrexate's limitations is the toxic side effects. Some studies have improved methotrexate formulations for topical treatment of skin diseases.[65]

Cyclosporine (or cyclosporin A) has been clinically used for the treatment of inflammatory and autoimmune diseases, including skin disorders like psoriasis [66] and severe atopic eczema.[67] Topical delivery of cyclosporine is a promising strategy to treat skin disorders, since it avoids several side effects associated with systemic delivery.[66]

Stock solutions of the test compounds were prepared by dissolving the drug in phosphate buffer pH 7.4 (for methotrexate and cyclosporine with addition of 10% (v/v) DMSO and 20% (v/v) ethanol, respectively) on a sonication bath (Sonica® Ultrasonic Cleaner). The caffeine, naproxen, diclofenac, methotrexate and cyclosporine concentrations were 0.52, 0.012, 0.5, 0.5 and 0.18 mg mL^{-1} respectively.

These compounds were applied in the mixture with calcein solution and the changes of calcein permeation was evaluated by measuring its fluorescence in the presence of each studied drug with wide range of the physicochemical properties. For each studied drug a 20% (v/v) stock solution in 1 mM calcein solution was added in the donor chamber, with means that the studied concentrations were 104 µg mL^{-1} for caffeine, 2.4 µg mL^{-1} for naproxen, 100 µg mL^{-1} for diclofenac, 100 µg mL^{-1} for methotrexate, 36 µg mL^{-1} for cyclosporine. All solutions were freshly blended before the calcein permeation studies.

2.6 Permeation studies for human *SC* model

Before the permeation experiments, the freshly prepared *SC* models were incubated with the buffer (PBS or HEPES for phospholipid quantification assay only) for 15 min.[68] The inserts were placed in the individual acceptor compartments in 24-well plate containing 2 mL of PBS or HEPES (pH 7.4) for each cell and were fixed (Fig. 13). The contact with buffer promoted a better saturation of the liposome layers. Permeation studies were performed after adding 1mM calcein solutions (alone or with addition of described compounds) in the inserts.

Fig. 13 – The experimental set-up used in the calcein permeation studies

The permeation experiments were carried out at room temperature without agitation (for all experiments besides phospholipid quantification assay) and with protection from light. The inserts were moved by tweezers to wells containing an equal quantity of fresh buffer (2 mL) at 30 min intervals for 3 h of study. At the end of the experiment, samples (300 µL) from each acceptor compartment were transferred into 96-well black plates and analyzed at 20°C in a microplate reader with excitation and emission wavelengths at 485 nm and 528 nm, respectively.[6, 36]

For the permeation studies with co-solvents, DMSO, oleic acid and cremophor® were used. The concentration of co-solvents was 10% (v/v) in calcein solutions. The mixtures were vortexed for 1 min and immediately loaded on the donor chamber.[69]

The permeation assays were conducted under a pH range from 2.0 to 8.0 with 1 mM calcein solutions for pH 2.0, 7.4 and 8.0 (pH adjustment with HCl/ NaOH to the necessary value) in the donor cell and PBS (pH 7.4) in the acceptor chamber [6]. The influence of pH changes in the permeability of acidic and basic drugs was determined by using 100 µg mL^{-1} methotrexate (pH 2 and pH 8) and 104 µg mL^{-1} caffeine (pH 2 and pH 8) in the calcein solution. The acceptor compartment contained PBS pH 7.4.[69]

The stability of the membranes during storage at two different temperatures (-20°C and -80°C) up to two weeks was evaluated by performing permeation experiments using 1 mM calcein solution.[6]

The transepithelial resistance (TEER) of the lipid barriers was measured (EVOM2®, Epithelial Volt/Ohm (TEER) Meter with STX2 electrodes, which contains a silver/silver-chloride

pellet for measuring voltage and a silver electrode for passing current, World Precision Instruments) directly after the end of permeation studies.[38]

2.7 Permeation studies with Franz Diffusion Cells

2.7.1 Pig skin preparation

The young white porcine ears from different animals were initially cleaned and dried with soft paper, then the exterior skin was removed from the underlying cartilage using a knife. The subcutaneous fat tissue was cut off by a scalpel cautiously to keep the integrity of the pig skin. Porcine skin samples were gently dry-shaved if necessary, when not used immediately. The skin was packed in aluminum foil, marked and stored at 4°C up to 2 days or at -20°C up to 2 weeks. These samples were kept at room temperature for 30 min before being used in the experiment.[70] For each experiment, the skin was divided in pieces with same thickness generally from central part of the ear skin, visually inspected to ensure its integrity, no content blood vessels and skin defects.

2.7.2 *In vitro* permeation studies

The skin permeation of the control calcein-containing solutions described above were evaluated using a Franz cell assembly (9 mm unjacketed Franz Diffusion Cell with 5 mL receptor, O-ring joint, clear glass, clamp and stir-bar; PermeGear, Inc., USA). Pig ear skin was placed between donor and acceptor compartments in the Franz diffusion cell and held in place with a clamp (Fig. 14).

Fig. 14 – Permeation studies with Franz Diffusion Cells

A volume of 0.5 mL of the test solutions with a known concentration were loaded in the donor chamber, the receiver chamber was filled with 5 mL of PBS (pH 7.4) and each cell was covered with Parafilm®. The diffusion area between cells was 0.64 cm^2.[70, 71] The Franz Cell system remained at room temperature upon 3 h of study. The acceptor compartment also contained a magnetic stir-bar, promoting stirring during 1 min prior sample collection. Aliquots of 0.5 mL were collected at time 0.5, 1, 1.5, 2, 2.5, 3 h from the sampling port and replaced with the same amount of fresh buffer.

All collected samples were analyzed by fluorescence measurement in the microplate reader with excitation and emission wavelengths at 485 nm and 528 nm, respectively. The quantification of the calcein concentration was obtained by the linear equation obtained from a prepared standard curve.

2.7.3 Permeability calculations

After fluorescence measurements, the concentration of calcein in the acceptor chamber was calculated using calibration curve. Mass of calcein in every lower compartment was accounted by next formula:

$$m_a(g) = C_a \cdot V_a \cdot M_w \quad (1)$$

where C_a is the calcein concentration in the acceptor chamber (M), V_a is the volume of the lower chamber ($2 \cdot 10^{-3}$L) and *Mw* is the molar mass of calcein (622.55 g mol^{-1}).

For the permeation studies with Franz Diffusion Cells similar calculations were performed. Mass of calcein was computed for each sampling aliquot (0.5 mL), for last volume of acceptor cell (5 mL) and finally summarized.

The obtained masses were then used to estimate the apparent permeability coefficient (P_{app}) by use following equation:

$$P_{app}(cm/s) = \frac{\sum m_a}{A \cdot m_d \cdot t} \quad (2)$$

Where sum of m_a is the mass of calcein permeated across membranes in acceptor chamber (g), *A* is the surface area of the inserts (0.6 cm^2) or the diffusion area between cells in

Franz diffusion system (0.63585 cm^2), m_d is the initial mass of calcein in donor chamber (g) and *t* is the time (3 hours = 10800 s).

2.8 Scanning Electron Microscopy

To investigate the surface topography of the phospholipid vesicular membranes, the Scanning Electron Microscopy (SEM) technique was used. SEM scans the surface with a focused beam of electrons. The electrons interact with atoms in the sample, producing different signals that contain information about the sample's surface topography and composition. SEM studies were performed by an Ultra-High Resolution Analytical Scanning Electron Microscope HR-FESEM Hitachi SU-70, designed to work though the ultralow landing voltage. The *SC* models were prepared in the usual way, the membranes were cut out from support and placed on a sample's holder. The 1 kV landing voltage was used for observing soft surfaces without covering.

2.9 Phospholipid quantification assays

The liposome preparation and calcein permeation studies were performed only with buffer HEPES (pH 7.4). The agitation was used during the permeation assays for two phospholipid vesicular membranes. 0.4 mL of an aliquot from the receiver chamber for last point (3 h) was dried in a Pyrex tube in the oven at 120°C. The standard curve tubes were treated in the same manner.

The Pyrex tube was placed in a beaker containing paraffin oil. Perchloric acid (0.4 mL, 70%) were added, covered each tube by marbles to prevent loss of perchloric acid fumes (Fig. 15) and heated for 1 h at 180°C for mineralization on the ceramic heating plate (IKA Magnetic Stirrers, C-MAG HS 7 Package) with connecting a contact thermometer (ETS-D5, IKA Hot Plates Accessories).

Fig. 15 – Phospholipid quantification assays setup

After cooling, the reagents were added in order: water (1 mL), 1.25% (w/v) ammonium molybdate (0.4 mL), and 3% (w/v) ascorbic acid solution (0.4 mL). The additions were made rapidly and the tube contents were mixed after each addition with a vortex. All the tubes were boiled at 100°C for 5 min on the ceramic heating plate. The absorbance was measured at 797 nm in a V-660 UV-VIS Spectrophotometer (JASCO Germany Labor). To obtain standard calibration curve, Monopotassium phosphate (KH_2PO_4) solution 1 mM was used.[72]

2.10 Statistical Analysis

Results are reported as a mean ± standard deviation from a minimum of three independent experiments. The Student's t-test (two-tailed) was used to evaluate the statistical significance of any differences in mean values in experimental groups. Differences were considered significant at $p < 0.05$. Statistical analysis was computed using GraphPad Prism Software (Version 6.01 for Windows; GraphPad Software Inc, San Diego, CA, USA).

III RESULTS AND DISCUSSION

3.1 The structure of the phospholipid vesicle-based *SC* model

This work aimed to produce a *SC* model, which more closely mimic the human *SC* based on a specific chosen liposome composition, to further estimation of skin permeability. Thereby, the first step was to examine the structure of the designed and prepared phospholipid vesicle-based barrier. To achieve this purpose, the following techniques were employed:

- DLS to assess the size of both types of liposomes used in the model;
- scanning electron microscopy to visualize the surface of the phospholipid vesicular barriers;
- phospholipid quantification assay to determine the stability of the barrier.

Different size of liposomal structures was used to promote the spreading into the pores and onto the membrane surface.[36] This hypothesis is based on previous literature data: the liposome extrusion makes the vesicle's sizes conformable to the size of the filter pores.[73] Also, the repetitive extrusion cycles through the same filter have been shown to decrease the liposome size.[74] The skin *SC* model was produced by first adding smaller liposomes which pass into the pores, and then larger liposomes that made an expected layer on top of the membrane filter.[6]

3.1.1 Determination of size and polydispersity of the liposomes

The liposome suspensions were produced as multilamellar large vesicles (MLVs) with a main size distribution in the range of 800-1200 nm and LUVs with mean diameter 100-400 nm. In order to gather data about the diameters and polydispersity (PDI) of each liposome batch used in the present study, the DLS technique was employed. The collected results are summarized in Table 9.

Table 9 – Characterization of the liposomes populations

Parameters	MLVs	LUVs
Effective diameter (nm)	979 ± 84	251 ± 34
Polydispersity index (PDI)	0.37 ± 0.01	0.24 ± 0.02

Data expressed as mean ± standard deviation (n = 10).

The MLVs exhibited an average size of 979 ± 84 nm, which makes them possible to apply on top of the inserts. The MLVs demonstrated a bimodal size distribution, that is, two clear vesicle populations could be detected. The mean size of the main fraction, which contained more than 55% of the liposomes, was approximately 535 nm, and that of the smaller fraction, containing less than 45% of the liposomes, was approximately 3615 nm (Fig. 16A). In agreement, all the MLVs prepared in this study showed relatively large polydispersity index (PDI) values (0.37 ± 0.01), which indicates a heterogeneous distribution of vesicles of many different diameters.

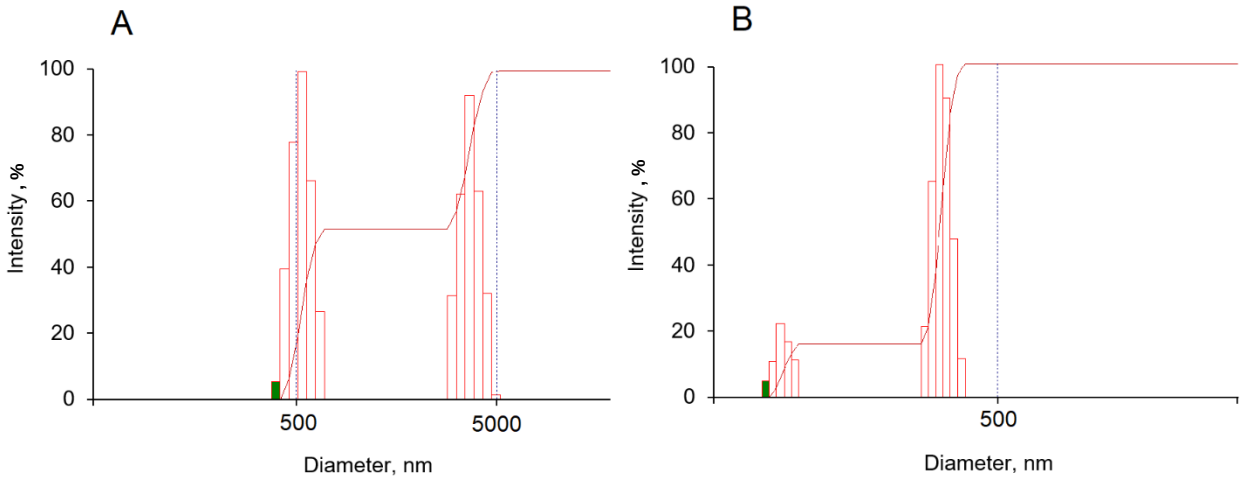

Fig. 16 – Size distribution of vesicles used in this study measured by DLS. (A) MLVs; (B) LUVs

The LUVs displayed an average size of 251 ± 34 nm. They are smaller than the MLVs, as expected, and suitable to fill in the membrane pores. The LUVs also showed a bimodal size

distribution, 103 nm (20%) and 354 nm (80%), which is shown in Fig. 16B. The PDI is 0.24 ± 0.02, slightly higher than 0.2, indicating a more homogeneous range of liposome sizes.

For the purpose of comparison, we determined the mean diameters of the liposomes, which passed through the filter during the preparation of *SC* model, and for that, were not incorporate within the phospholipid-vesicular based membrane. It was 198 ± 8 nm (n=2).

In sum, regarding the results for particle size, LUVs demonstrated smaller average size (251 ± 34 nm) that allow them to congestion inside membrane pores (400 nm), and MLVs had bigger diameter (979 ± 84 nm), which doesn't allow to penetrate throughout the membrane barrier, but makes possible to form a tight liposome layer on top of the membrane surface. Thus, the phospholipid vesicular barrier preparation process followed accordingly: first, a portion of the liposomes pass via the membrane filter (the liposomes were found in the infiltrate by microscopy), but after the several steps, the pores are filled with LUVs and a layer on the top begins to form by MLVs. At the end, the membrane loses its initial throughput capacity, a supernatant is formed and finally the barrier model can be obtained.

3.1.2 Scanning electron microscopy analysis

The surface morphology of the *SC* models was examined by scanning electron microscopy (SEM). SEM analysis was performed with low-landing voltage to visualize the liposome layer and the micrographs are shown in Fig. 17. The images present the phospholipid vesicular barriers with different storage conditions: the recently prepared barrier model (A-C) with various magnifications and the membrane model stored for about 4 months at 4°C (D).

SEM micrographs confirmed that the *SC* model have a tightly, non-porous surface, which completely covers the filter (Fig. 17A). On the next image (Fig. 17B) an uneven surface with small round-shape particles, hypothetically, liposomes vesicles and some crystals of phosphate buffer can be observed. Even at very high magnification, it is possible to observe that the liposome layer is coating the filter, the pores are not discovered, and a border of detached layer is also visible (Fig. 17C). Moreover, it is worth noting that this image had some similarities with micrograph of human *SC*, obtained from previous studies (Fig. 18).[7]

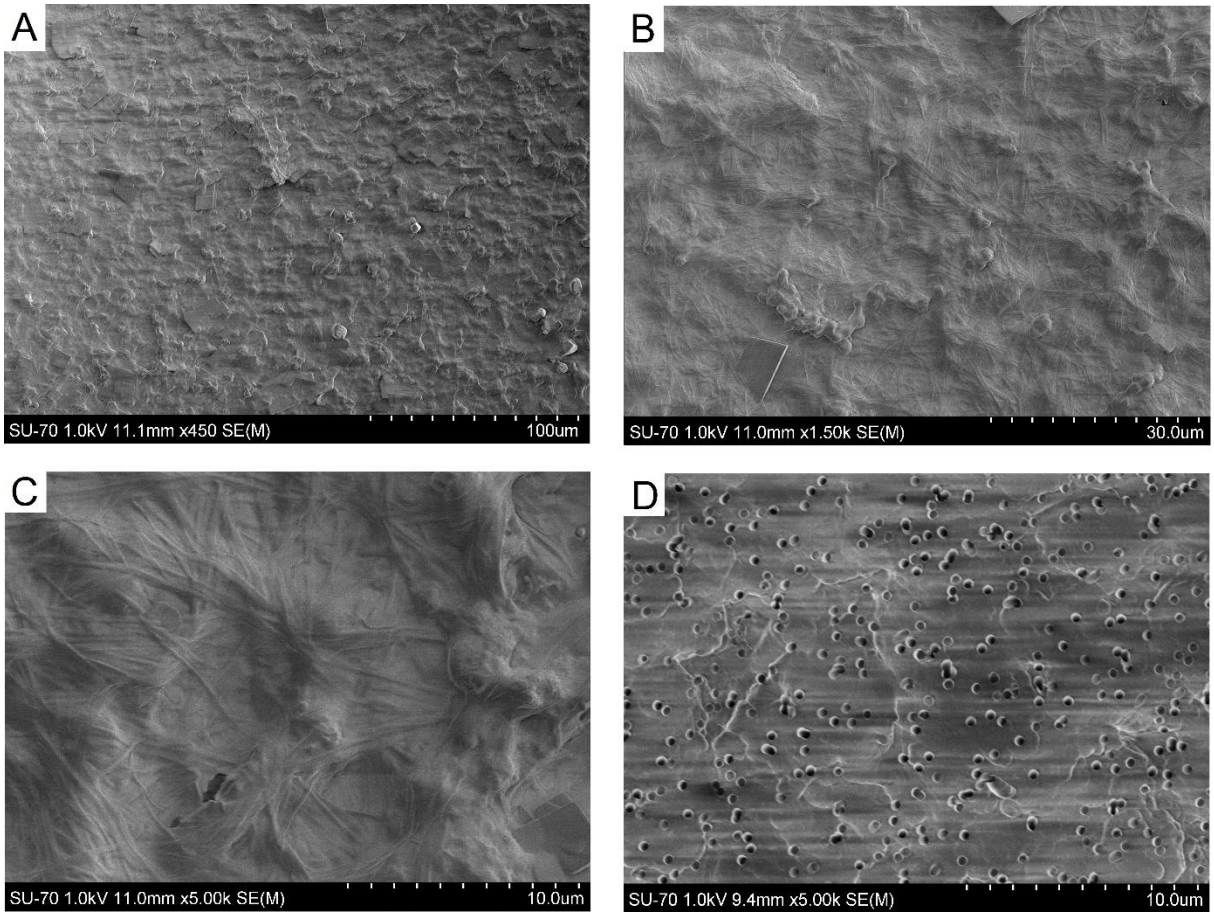

Fig. 17 – SEM images of (A-C) freshly prepared, and stored for 4 months at 4°C (D) the phospholipid vesicular barriers. The scale bar is indicated below images

A large amount of pores is presented on the surface of the barrier upon 4 months stored (Fig. 17D). We can probably assign as the absolute absence of the liposome layer because we can observe the pure filter and the initial pores (diameter is 400 nm). This fact is related with the stability studies described below.

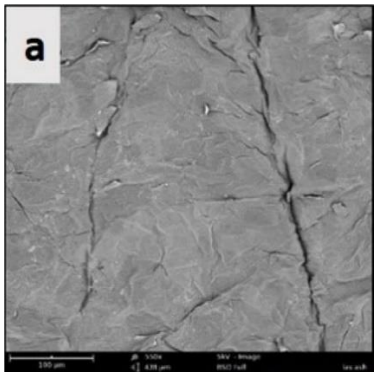

Fig. 18 – SEM images of untreated human skin[7]

3.2 Characterization of the phospholipid vesicle-based model

3.2.1 Calcein permeability and electrical resistance

In order to get significant data from the permeability assays, a confirmation of the *SC* models was carried out by two independent assessments: testing the penetration of hydrophilic fluorescent marker (calcein) and the transepithelial electrical resistance (TEER) to validate the integrity of the barriers. Calcein was chosen as reference compound with pKa 6.67 [48], which presented a weak acid ionized form at working with pH 7.4 and showed good ability to diffuse across liposome layer in the barriers. TEER is commonly considered as a good indicator of barrier tightness.[50] The electrical resistance was measured after each permeation experiment i.e. after 3h incubation in the sample solution. The control measurements were performed by using the pure membrane filter (Fig. 19).

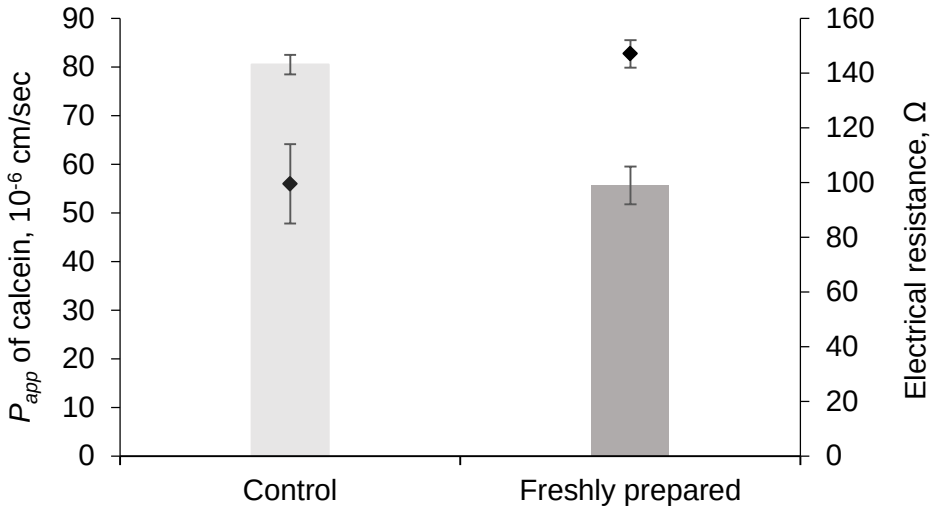

Fig. 19 – The permeability of calcein for the pure filter inserts (control) and freshly prepared phospholipid vesicular barriers. The electrical resistance is marked by the diamond dots. The values denote the mean ± S.D. (n = 3)

In the case of freshly prepared *SC* models, values for calcein permeability and TEER, were significantly lower and higher, respectively, when compared to pure control inserts. The results confirm the barrier integrity of the prepared models. Besides the increasing in calcein permeability and decreasing in TEER of the control values are assumed to exclusively reflect leakage of the pure membrane filter.

Nevertheless TEER- and calcein permeability-values are rather dissimilar from earlier published data for the *SC* model.[6, 69] Probably this can be connected with the case that the other

lipid composition, the filter area is smaller, acceptor volume here are bigger than in the earlier reported set-up. Also, the sensitivity of the electrode is not constant, the thickness of liposome layer is not analogous with previous studies, which were performed in same conditions in a one research group. [6]

However, in the current experimental arrangement, it could be concluded that in terms of calcein permeability and TEER, the integrity of the phospholipid vesicular barriers is maintained.

3.2.2 Phospholipid quantification

To verify the barrier integrity during the calcein permeation studies, the presence of phospholipid in the acceptor chambers after 3 h incubation in HEPES buffer was explored. The amount of phosphorous in the acceptor chambers was quantified by spectrophotometric determination. Briefly, the samples probably containing phosphate are converted to inorganic phosphorus by mineralization, then the phosphorus react with ammonium molybdate to produce $PMo_{12}O_{40}^{3-}$. This anion is then reduced by ascorbic acid to form the blue colored phosphomolybdic complex (molybdenum blue).[75] Nevertheless, a blue color was not observed and measured absorbance at 797 nm shown values at the range 1.1 – 1.9%, which indicates the lack of phosphorus.

No egg phosphatidylcholine could be detected in the acceptor phases, that confirmed the barrier integrity during the calcein permeation assays in terms of release of phospholipid and that is consistent with previous study.[69]

3.2.3. Storage stability

The storage stability of phospholipid vesicular barriers was estimated as a weighty argument in cost efficiency analysis of the drug development process. If *SC* models don't lose their permeability properties during a certain period of time, the cost minimization and an effortless planning can be reached by producing larger batches.

The stability of the barriers upon keeping at two various temperatures was assessed by evaluating the calcein permeation after different storage times. The calcein permeability (P_{app}) values received from the developed *SC* models stored at the various temperatures are presented in Fig. 20.

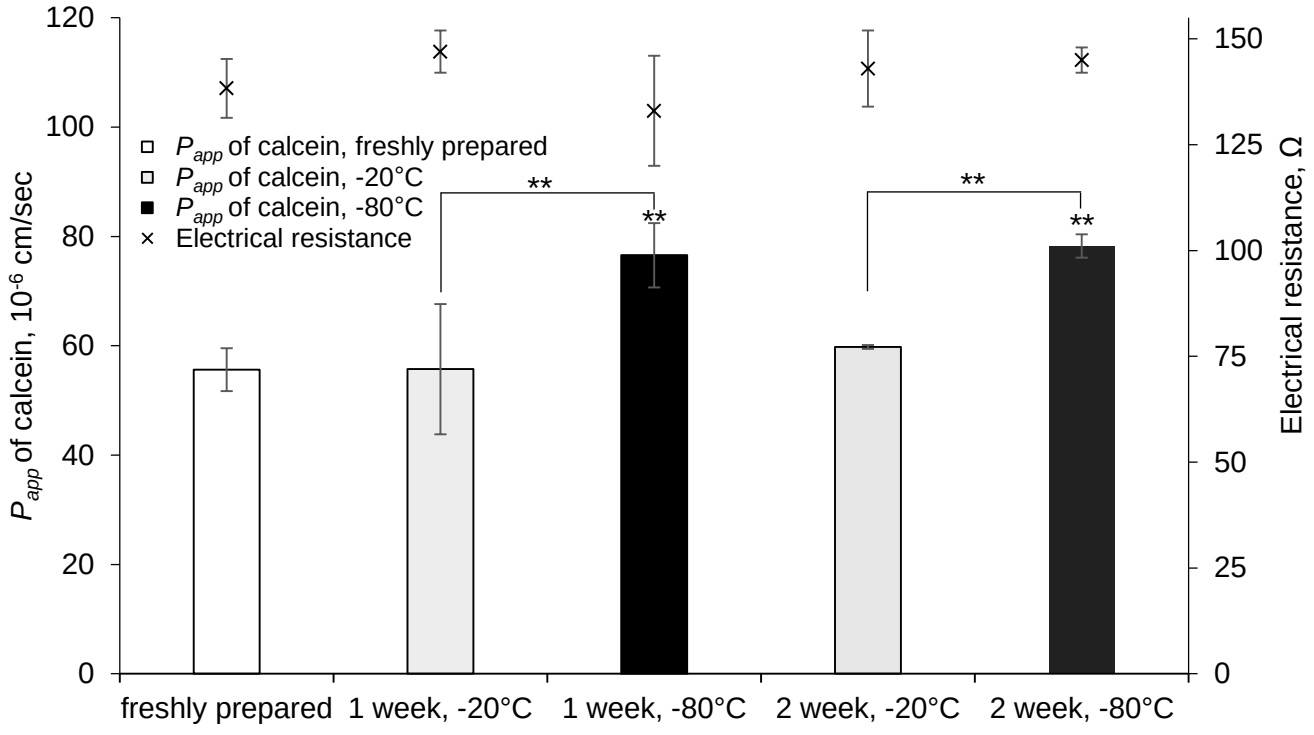

Fig. 20 – Effect of storage conditions: -20°C and -80°C on calcein permeability and electrical resistance through the phospholipid vesicular barriers. Error bars represent the standard deviations (n=2 and for freshly prepared n=4). ***P*<0.01 in relation to freshly prepared membrane (control)

As can be seen from the results in Fig. 20, the permeability did not significantly differ from those of the control (freshly prepared) for up to 2 weeks of storage at -20°C. These conditions show great promise without any considerable variations with respect to the permeability of calcein.

On the contrary, a 25% increase in the permeability of calcein was observed after 1 and 2 weeks of storage at -80°C. The results of the evaluation of phospholipid vesicles barrier using calcein are likewise as previously published stability results for PVPAs, which also designated a limit of 2 weeks of storage at -70°C.[36, 39] This dissimilarity in the storage temperature can be explained based on the *SC* barrier more complex lipid composition, which showed more sensitiveness for low temperatures.

In summary, the *SC* models can be prepared in larger batches, and be saved in a freezer and will be ready to use after 2 h of thawing on any day during the recommended period of storage.

3.2.4 Barrier stability under a pH range 2.0 to 8.0

The barrier stability under different pH conditions can provide information on the applicability of the developed phospholipid vesicle barriers in the screening for drugs in a wide range of pKa. The stability of the *SC* models towards changes in pH in a range from 2.0 to 8.0 was examined by the determination of calcein permeation under various pH values in the donor chamber. The acceptor chamber contained PBS buffer at pH 7.4. The permeability (P_{app}) of calcein under distinct pH conditions are presented in Fig. 21.

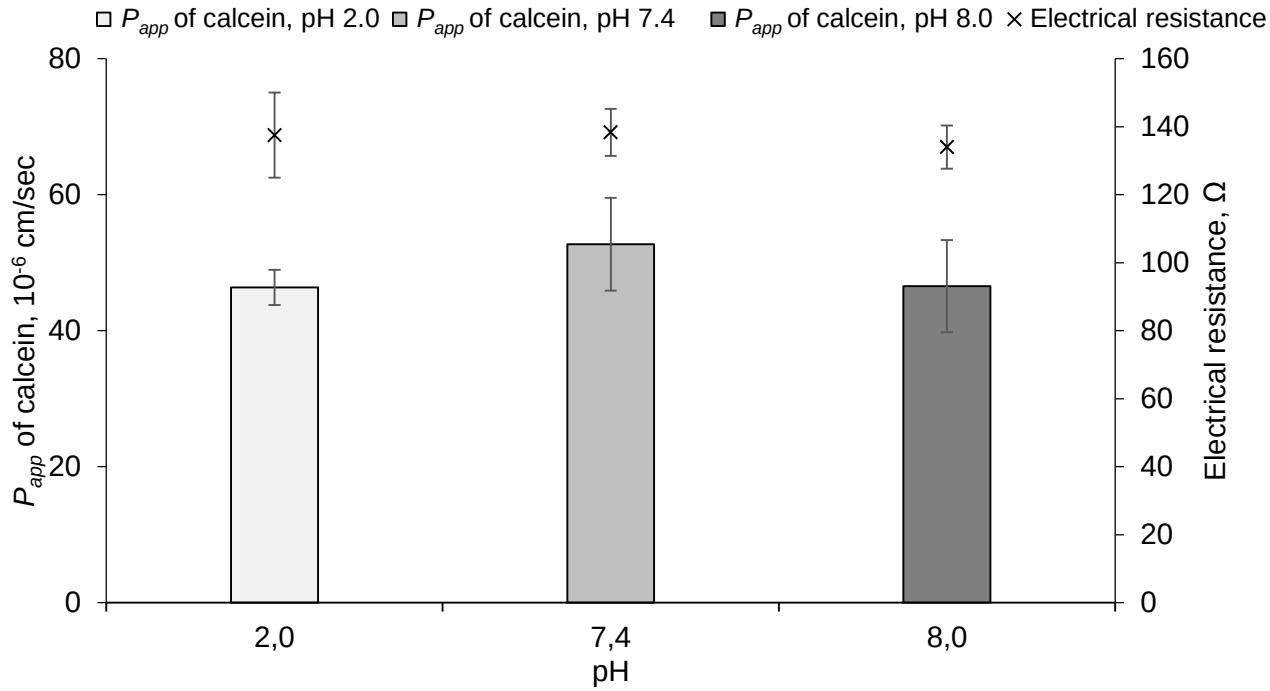

Fig. 21 – The P_{app} and TEER values of calcein at pH 2.0, 7.4 and 8.0. Data expressed as mean values ± SD (n=5)

The developed *SC* models seemed to be stable due to the unaltered permeability of calcein over the pH range explored. It is in agreement to earlier reported experimental results of fluorescein permeability for PVPA membranes.[6] Thereby, the prepared phospholipid vesicle

membranes do not forfeit their wholeness at pH margins from 2.0 to 8.0 and can be used for the screening of drugs with acidic and basic properties.

3.3 Characterization of drug–membrane interactions

3.3.1 Use of pH changes to influence the permeability of acidic and basic drugs

As described above, the integrity of the *SC* models is persisted at the pH range from 2.0 to 8.0 that allow the permeability studies of ionogenic drugs dependent on pH changes. Thus, the calcein permeability with caffeine and methotrexate (MTX), basic (104 µg mL^{-1}) and acidic (100 µg mL^{-1}) drug compounds, respectively, was tested at two different pH (2.0 and 8.0). The pH in the donor chamber was maintained at pH 7.4. The P_{app} values are given in Fig. 22.

From the chart, the permeability of calcein in the presence of MTX decreased with increasing the pH, for caffeine no significant effect was observed. For MTX the reduction in permeability was significant from pH 2.0 to 7.4 and from pH 7.4 to 8.0. For caffeine, the permeation results likely depend on the low amount of uncharged molecules at both these pH values, as caffeine has a pKa value of 14.0. As caffeine is a basic drug and MTX an acidic drug (pKa 4.7) this indicates that the permeability is slightly reducing with enhancing degree of ionization of MTX.

Most drugs are weak acids or weak bases, in which the relation of the charged (ionized) to uncharged (nonionized) form is contingent on the drug's pKa, and the pH of the surroundings. At same pH and a drug's pKa, the protonated and nonprotonated forms are in the equilibrium. If the pH is less than the pKa (the redundant protons are present), the protonated form of a drug prevails.[48, 76] Therefore, weak acid (MTX) subjected to low pH environment (pH 2.0) is preferred to diffuse across barriers while, weak bases are not, that is confirmed by the increased permeability shown on Fig. 22. This process has an opposite effect at higher pH (pH 8.0).

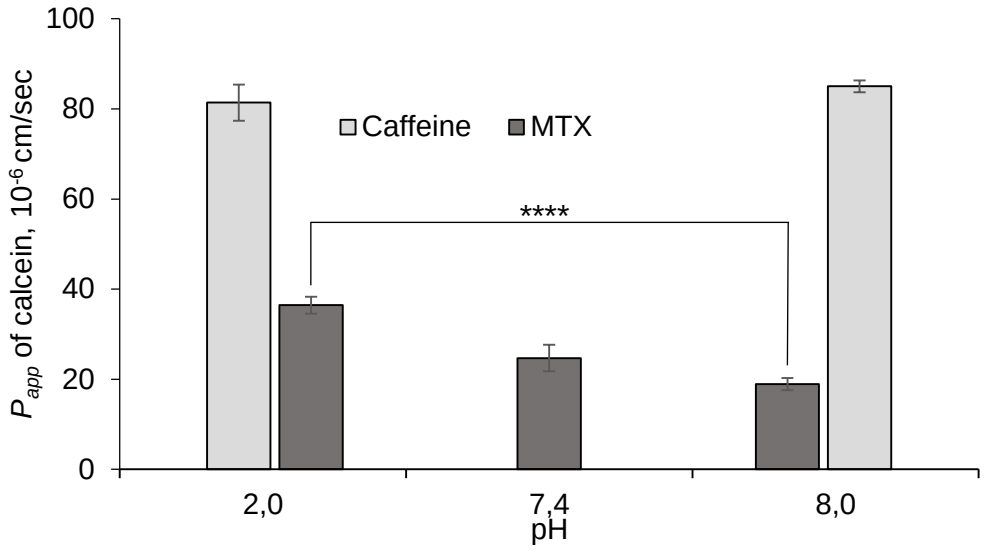

Fig. 22 – The permeability (P_{app}) values for caffeine and methotrexate (MTX) at pH 2.0, 7.4 and 8.0 in the apical medium and pH 7.4 the basolateral medium (n=3). ****P<0.0001 between MTX pH2 and MXT pH8

The discovered changes in calcein permeability with drugs reflect changes in the drug's ionisation state, but not of pH-dependent changes in the phospholipid vesicles barriers since the *SC* membranes are stable this pH interval. Our results also comply with the previous studies.[69]

3.3.2 Influence of surfactants and co-solvents in the phospholipid vesicle-based model

In this assay, it was examined the suitability of the *SC* model for permeability evaluations in the presence of surfactants and co-solvents. This was reached by measuring the stability of the phospholipid vesicular barriers in the presence of surfactant and co-solvents from point of view of calcein permeability and TEER.

Some drugs are insoluble in aqueous-based solvents, therefore various co-solvents were used for the design and optimization drug formulation for TDD.[77] DMSO and oleic acid are well known skin permeation enhancers [78], cremophor® is non-ionic surfactant.[79] DMSO is a potent aprotic solvent and can be contributing for topical delivery for various drugs.[78] DMSO is connecting with the intercellular lipid region of *SC* and meddling in the packing geometry, that promotes increment of skin permeability.[80] Oleic acid is the most popular of long chain fatty acids, which can enhance the drug absorption via the skin.[78] Oleic acid treatment contributes the reduced ability of skin barrier function by making a new type of lipid domain together with

SC lipid, that works as a skin penetration enhancer.[81] Cremophor® is a frequent component, which is using in the low-water soluble drug development.[82]

The testing of the integrity of the *SC* models was carried out by determining the calcein permeability in the presence of DMSO, oleic acid and cremophor® with concentration 10% (v/v) with calcein solution in the donor chamber for each compound. TEER measurements were performed after completed studies. The results are given in Fig. 23.

The results in Fig. 23 show that the presence of DMSO, oleic acid and cremophor® in the solution in the donor chamber did not influence the permeability of calcein at the studied conditions, as the results are not statistically different. The electrical resistance confirmed the integrity of the phospholipid vesicles barriers. According to the results for cremophor®, a little diminution of TEER with increasing permeability of calcein was found, but statistical analysis confirmed that no statistical differences in relation to calcein compound alone. The data has the correlations with published paper.[69] Thereby, the phospholipid vesicle membranes seemed to be reconcilable with DMSO, oleic acid and cremophor® for a concentration of 10% (v/v). They are not disrupting the structure of the barrier, which renders them suitable as additives in this model. Thus, the *SC* models are adequate for the development and optimization of the drug formulations in TDD using the listed surfactants and co-solvents compounds.

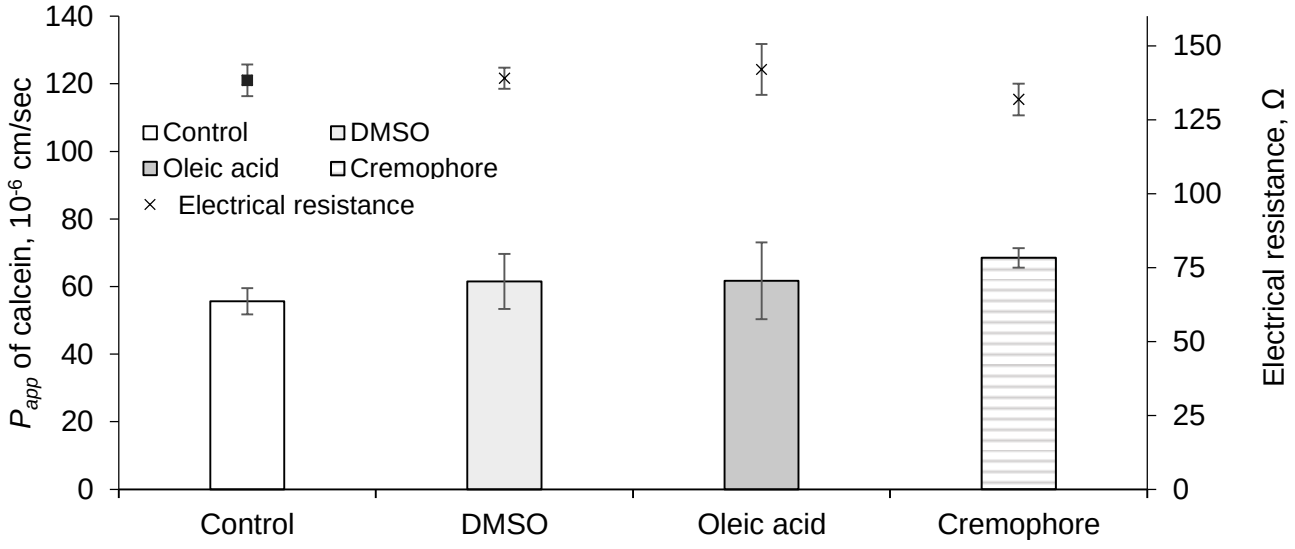

Fig. 23 – The permeability (P_{app}) values for calcein in absence (control) and presence of different co-solvents and surfactant in the donor compartment. Error bars denote the standard deviations (n=3)

3.3.3 Influence of drug substances on the *SC* model

Estimating the drug permeation via the skin is indispensable in the design of (trans)dermal delivery drugs. The developed *SC* model can be validated by evaluating the permeability of different drugs.

Preliminary assays have shown that some drug compounds can influence the calcein permeability (see Fig. 22), here's why permeability experiments with the hydrophilic marker calcein together with caffeine, naproxen, diclofenac, MTX and cyclosporine respectively, were made to consider if the drugs interact with the barrier and how they could influence the permeability of a calcein. The results from the permeability experiments with calcein under the presence of caffeine, naproxen, diclofenac, MTX and cyclosporine are shown in Fig. 24.

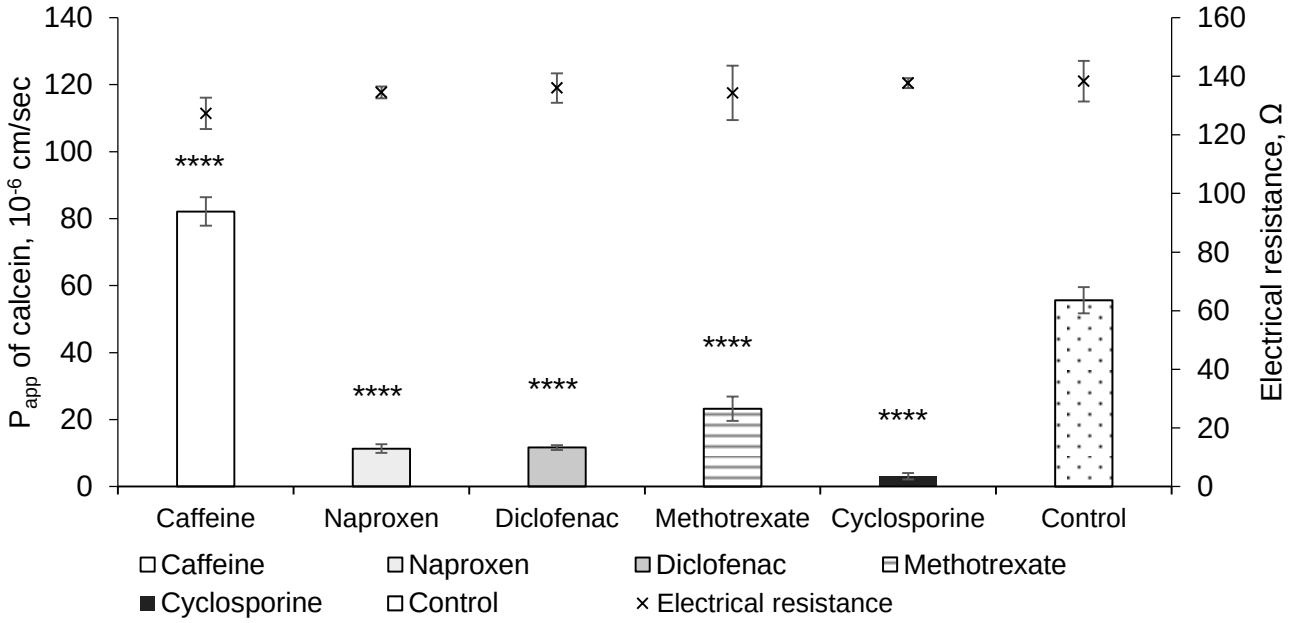

Fig. 24 – The permeability (P_{app}) values for calcein (bars) and the electrical resistance (x) across the SC model in absence (control) and presence of caffeine, naproxen, diclofenac, MTX and cyclosporine. Each result represents the mean ± standard deviation for n=3 measurements. ****P<0.0001 in relation to calcein alone (control)

It was found that all drugs had an influence on the calcein permeability. The permeability of calcein increased to a large extent when caffeine was present and decreased when other drugs

were present in the donor compartment. These changes possibly related to the chemical properties and structure of the drugs.

Caffeine is a small hydrophilic molecule, which increased the calcein permeability via phospholipid vesicles membrane because it has low affinity with the lipid layer and low molecular weight (Mw = 194 g mol^{-1}), that did not block its passage. Also, TEER measurements showed that electrical resistance decreased slightly, with no statistical meaning.

On the contrary, MTX is a lipophilic drug with medium interactions with lipids and Mw = 454 g mol^{-1}, which longer stays on the liposome layers, that corresponds to lower permeability values compare to calcein alone.

For cyclosporine, there was observed a considerable diminution in permeability of calcein, that can be linked with the highest molecular weight (Mw = 1203 g mol^{-1}) from the selected drugs and hydrophobic character. Cyclosporine has high affinity with the lipid surface and the big size molecules can block free transition of calcein solution throughout the *SC* membrane filter.

A reduction in the permeability of calcein was also noticed for naproxen and diclofenac, but not to the same extent as for cyclosporine. The obtained values are very similar and possibly establish linkage between naproxen and diclofenac resemblances, such as molecular weight (230 and 318 g mol^{-1}, respectively), PSA, pKa, chemical structure and hydrophilic nature (Table 8).

Consequently, the developed *SC* model can be used to evaluate the nature of drugs and predict the permeability properties in early stages of drug development.

4 Comparison the *SC* model with pork skin model

The capability of an *in vitro* model to find little variations in the penetration of drug carriers or formulations and to give reproducible permeability results are of utmost importance. To demonstrate the usefulness of the phospholipid vesicles membranes in drug development and formulation optimization, a number of experiments using Franz diffusion cells and porcine skin as a barrier model were performed.

The studied conditions were identical to the previous experiments with the developed *SC* models in following parameters: same tested solutions, buffer, temperature and lack of agitation.

It is useful to note, one of the differences is using a full epidermis part of pork skin, not only *SC* layers, that's why we can observe some dissimilarities in the order of magnitude of P_{app} values.

4.1 Effect of storage conditions

The storage stability is one of most important factor in planning during drug development. The calcein permeability results for the *SC* model and porcine skin stored at 4°C and -20°C are presented in Fig. 25.

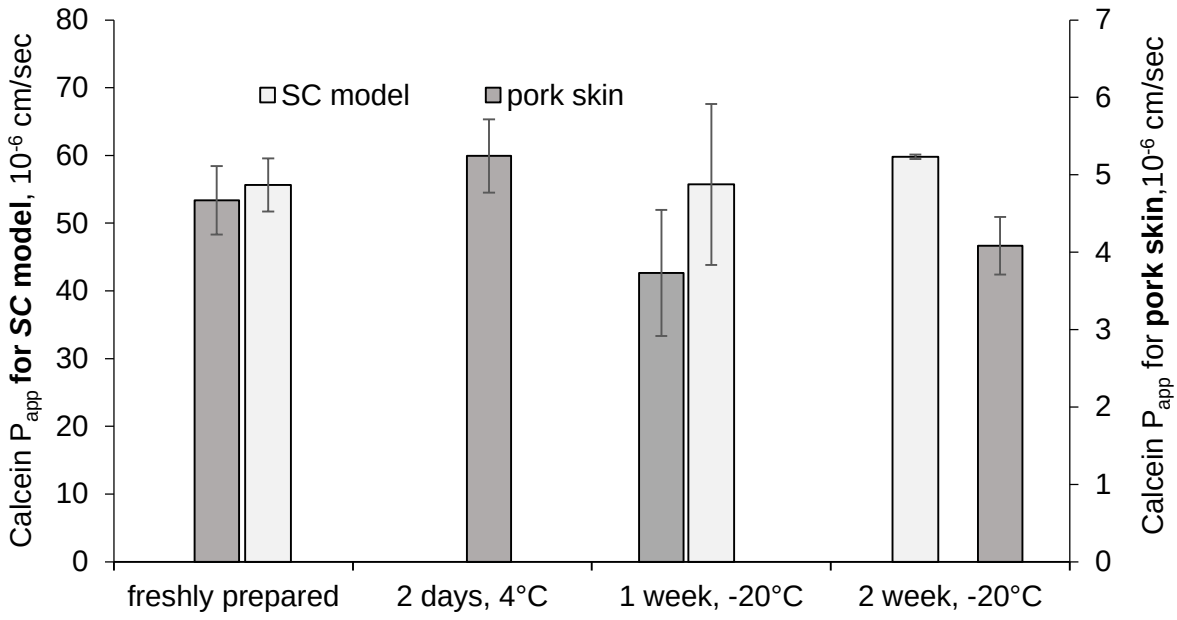

Fig. 25 – Correlation between the calcein permeability (P_{app}) values from *SC* models (n=2) and the obtained values from pork skin assay (n=3) in terms of storage stability. Error bars represent standard deviations

The results from the stability experiments with the pig ear skin using the Franz diffusion cells showed that the permeability of calcein was not significantly different from that of the control (freshly prepared) up to 2 days of storage at 4°C. However, a small reduction in the permeability of calcein was observed after 1-week of storage at -20°C. Low temperatures can effect on the permeability of pork skin (probably, by collapsing the pores) and on the enzyme system involved in metabolic process.[83] According to the described results, the storage of porcine skin is not recommendable at -20ºC.

At the same time, the phospholipid vesicles barriers can be stored up to 2 weeks at -20°C without any significant changes in the calcein permeability (Fig. 25), that is an important advantage in comparison with to the commonly used animal skin model.

4.2 Effect of various pH values (2.0 – 8.0)

The permeability studies at the pH range 2 to 8 were performed as described earlier (Section 2.6). In short, the calcein solutions with different pH (2.0, 7.4 and 8.0) were placed in the donor chambers. The acceptor chambers were prefilled with phosphate buffer (pH 7.4). The obtained results are shown in Fig. 26.

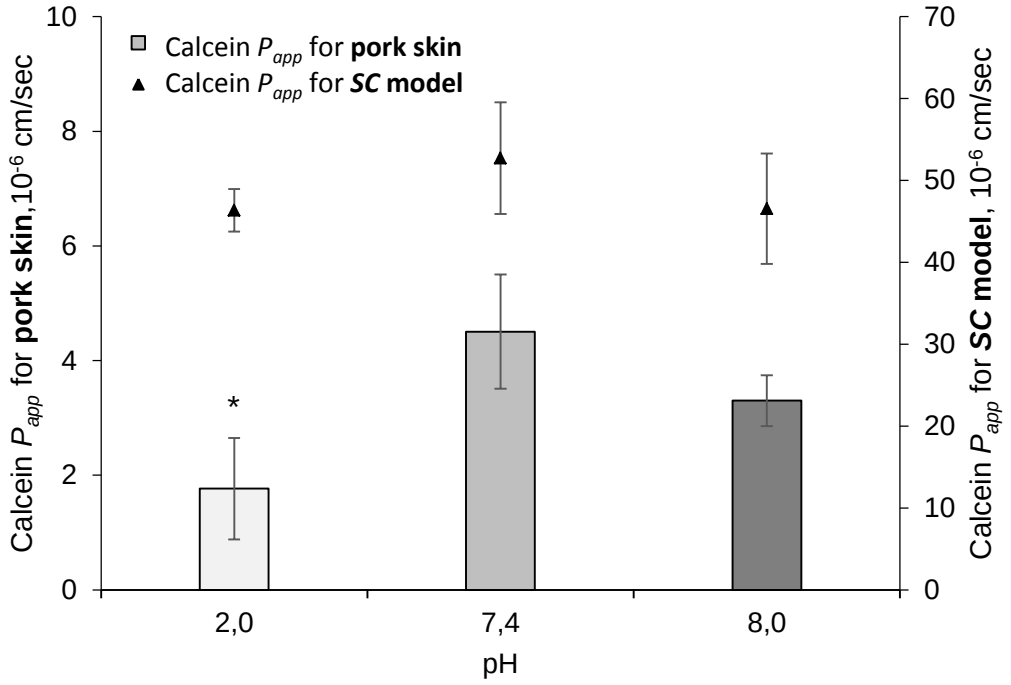

Fig. 26 – Correlation between the calcein permeability (P_{app}) values from *SC* models (triangles, n=3) and from pig ear skin model (bars, n=4) towards pH range from 2.0 to 8.0. *P<0.05 in relation to calcein permeability at pH 7.4 for pig ear skin model

The results on Fig. 26 show that the porcine skin was able to maintain the calcein permeability at the pH values 7.4 and 8.0. However, a significant statistical decrease ($P < 0.05$) in the calcein permeability was evident at pH 2.0. These data indicated that low pH values had an influence on the permeability of the pork skin, and the future evaluations at this pH can be give an erroneous result. While the developed *SC* model had correlations with used pig skin at

the pH range 2.0 to 8.0 that confirmed its ability for the permeation evaluation of a wide range of drugs.

4.3 The influence of co-solvents and surfactant

In the present study, DMSO, oleic acid and cremophor® were applied as additives to calcein solutions for the evaluation their influence on permeability of tested *SC* model and porcine skin model. Fig. 27 shows the permeability matching between the phospholipid vesicles barrier and pig ear skin model.

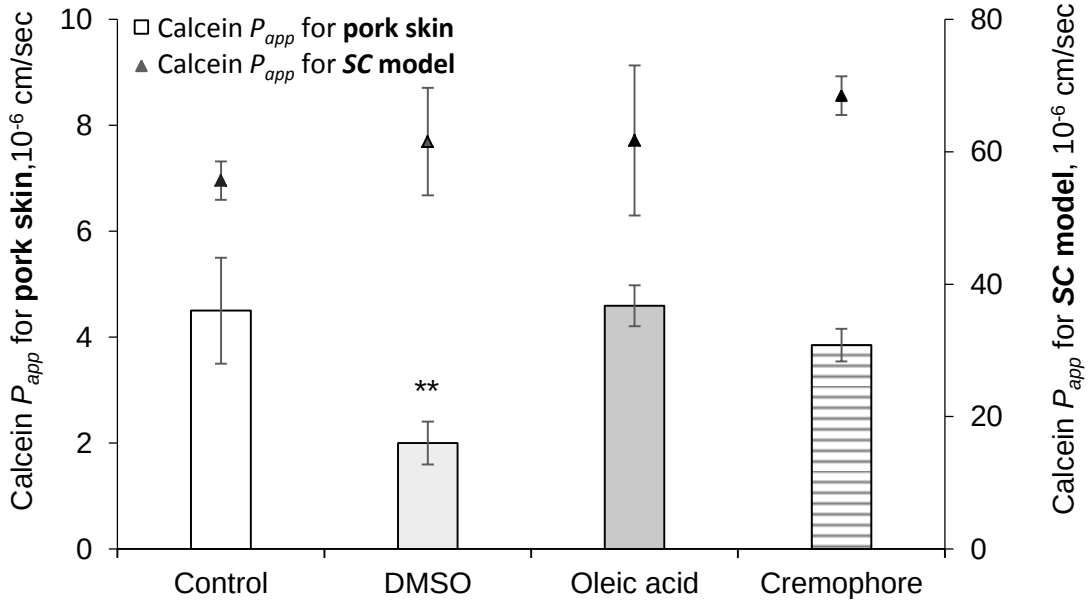

Fig. 27 – The calcein permeability (P_{app}) values from *SC* models (triangles) in comparison with P_{app} for pork skin from Franz diffusion cell assays (columns) in presence of the co-solvents (n=3). **P<0.01 in relation to control (calcein alone)

According to the information detailed in the Fig. 27, the pork skin doesn't maintain the initial calcein permeation with the addition of 10% (v/v) DMSO, but oleic acid and cremophor® don't affect the P_{app} of calcein. Therefore, for testing and optimization of drugs in the porcine model DMSO should be avoided as co-solvent.

The benefits of the developed *SC* model include the stability in the presence of the studied co-solvents and surfactant, which gives more opportunities in optimizing drug formulations.

4.4 Effect of acidic and basic drugs

To compare the effects of acid and basic drugs on the calcein permeability for the *SC* model and the pork ear model, at the pH range (2.0 - 8.0), the analogous calcein solutions containing caffeine and MTX additives were chosen. The results are presented in Fig. 28.

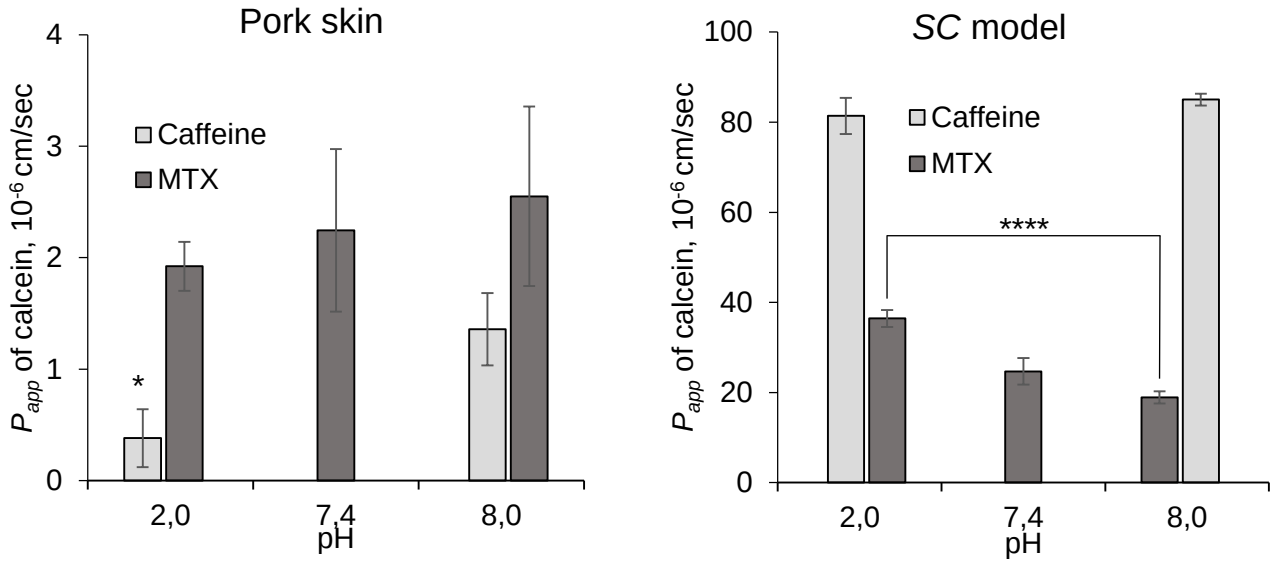

Fig. 28 – Correlation between the calcein permeability (P_{app}) from pig ear skin experiments (left side, n=3) and from *SC* models (right side, n=3) in the presence of the acidic (MTX) and basic (caffeine) compounds toward the pH range from 2.0 to 8.0. *P<0.05 in relation to caffeine pH 8 for pig skin model and ****P<0.0001 between MTX pH2 and MXT pH8 for *SC* model

The calcein permeability in the presence of MTX for pork skin (Fig. 28, left side) didn´t show meaningful changes at the chosen pH interval. The relation between pK_a and P_{app} do not occur, which can be explained by the influence of low pH on the porcine skin, which decreased the permeability (Fig. 26). The *SC* model is not liable to pH changes, and the correlation between pK_a and P_{app} are shown on Fig. 28 (right side), where significant differences (*P<0.0001) in P_{app} calcein with MTX can be observed. The permeability of the calcein with caffeine as addition at lower pH (2.0) demonstrated a considerable diminution (P<0.05) of P_{app} in relation the solution with higher pH (8.0). In fact, it is confirmed that the reduction in calcein permeability could be generated by lower pH value. We cannot make the conclusions about the influence of basic drug on calcein permeability towards pH range because of the described reasons.

4.5 The influence of drug substances

The permeabilities studies were performed with Franz diffusion systems and pork skin as a model barrier. The technique and conditions were an analogous to permeability assays with the phospholipid vesicles membranes. The control was a calcein solution without additives. The matching effects are indicated on Fig. 29.

All tested drugs had an influence on calcein permeability via pork skin, that were confirmed by substantial changes in the relation to pure calcein solution, which are designated on Fig. 29. The drugs were ranked based on their permeability values for the pork skin and *SC* models in decreasing order as follows: caffeine, naproxen, diclofenac, MTX and cyclosporine, that corresponded with their molecular weight.

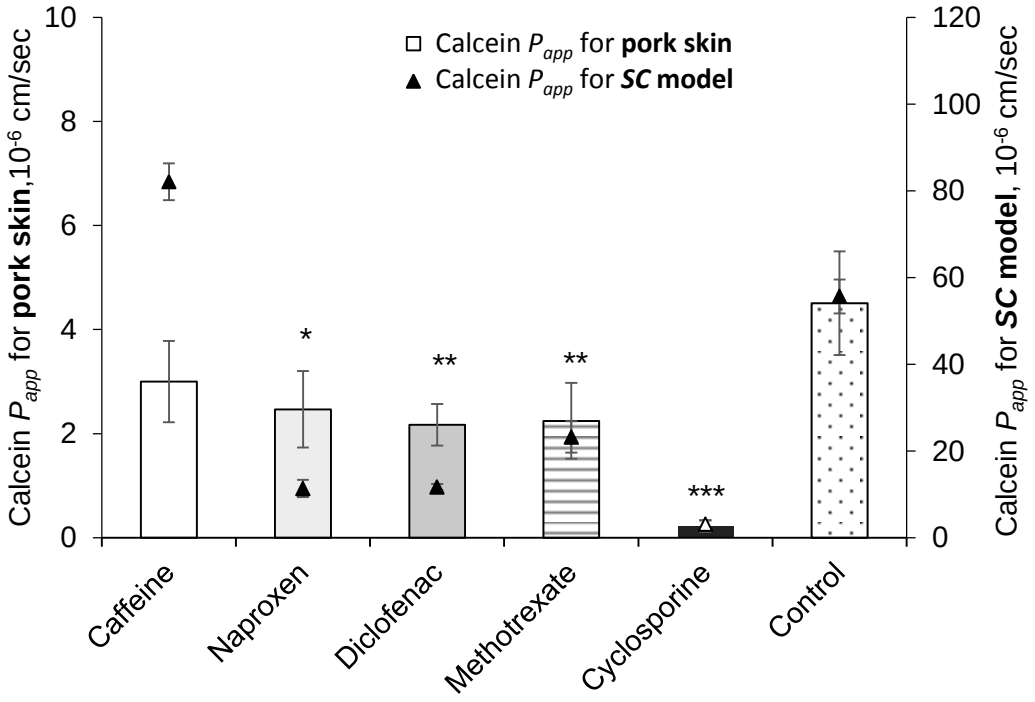

Fig. 29 – The permeability (P_{app}) values for calcein for pork skin (bars) and the *SC* model (triangles) in absence (control) and presence of caffeine, naproxen, diclofenac, MTX and cyclosporine. Each result represents the mean ± standard deviation for n=3 measurements. *P<0.05, ** P<0.01, **** P<0.0001 in relation to calcein (alone) for pork skin.

Thus, the highest Mw (cyclosporine) exhibited the lowest P_{app} value, and a correlation was observed for both the *SC* and the pig ear models. The cyclosporine is a big and very lipophilic molecule, which has strong affinity with lipid even at low concentrations (36 μg mL^{-1}).

The MTX is also lipophilic compound with molecular weight (454 g mol^{-1}) lower than cyclosporine molecule. The calcein permeability with MTX is lower than alone calcein because of the interaction with the lipid layers, and higher than calcein permeability in presence of cyclosporine owing to smaller size. These evidences were noted for either the *SC* model and the pork skin equally.

Diclofenac and naproxen have similar chemical properties, pK_a, PSA and lipophobic character here's why same permeability values were viewed in the Franz diffusion cell studies and with little shift in the prepared phospholipid vesicles barriers. These deviations can be accounted for the size of molecules, probably, block aqueous pores in the *SC* membranes that slightly reduce the calcein permeability.

Caffeine is a small drug with very hydrophilic properties, which showed higher calcein permeability compared with other drugs. The differences between the pork skin and the developed *SC* model can be explained based on the full-thickness of the skin epidermis that protects rapid penetration via skin for the caffeine molecules, in contrast with the phospholipid vesicles model, which mimicking only the *SC* layer.

IV CONCLUSIONS AND FUTURE PERSPECTIVES

With the results showed along this thesis, it is feasible to perform some final observations concerning the principal conclusions of these studies.

According with the first task, the goal was to design and characterize a human *SC* model. It is possible to claim that the chosen lipid composition allows to produce the phospholipid vesicles barriers, which mimic human *SC*. SEM images confirmed their structure, which presents similarity with human *SC*. Moreover, these barriers remain stable through 2 weeks at -20°C and show the stability towards pH range from 2.0 to 8.0 and to the presence of co-solvents and surfactant. Also, the developed *in vitro* model was able to detect permeability differences when the drugs were present in the calcein solutions and demonstrated a good correlation with chemical properties of selected drugs, especially with the molecular weight and an acidic/basic character.

Regarding the second purpose, the aim was to validate the developed model with the most commonly used animal skin model. Based on the data obtained from Franz diffusion cell experiments, it was possible to detect the relationship in the calcein permeability between the phospholipid vesicles membranes and porcine ear skin, that was clearly visible in the permeation studies with the additives of drugs. Besides, prepared *SC* models showed some advantages: better storage stability and an independence from pH and co-solvents.

Hence, the phospholipid vesicles barriers were found to be superior to pork skin by the described parameters and according to their ease of use, cost effectiveness and ability to replacement animal skin for permeability tests of potential drug formulations early in the development process.

Future experiments, which include wide range of drugs/chemicals and formulations without calcein solutions, need to be performed to prove the developed *SC* models' full capacity as a model for human *SC*.

References and citations

[1] Hunter, J. A. A., Savin, J. A., and Dahl, M. V. (2003) The function and structure of the skin, In *Clinical Dermatology* (Hunter, J. A. A., Savin, J. A., and Dahl, M. V., Eds.).

[2] Ovaere, P., Lippens, S., Vandenabeele, P., and Declercq, W. (2009) The emerging roles of serine protease cascades in the epidermis, *Trends Biochem Sci 34*, 453-463.

[3] Prausnitz, M. R., Elias, P. M., Franz, T. J., Schmuth, M., Tsai, J. C., Menon, G. K., Holleran, W. M., and Feingold, K. R. (2012) Skin barrier and transdermal drug delivery, In *Dermatology* (Bolognia, J., Jorizzo, J. L., and Schaffer, J. V., Eds.), pp 2065–2073.

[4] Uchida, Y., and Park, K. (2016) Stratum Corneum, In *Immunology of the Skin: Basic and Clinical Sciences in Skin Immune Responses* (Kabashima, K., Ed.), pp 15-30.

[5] Ng, K. W., and Lau, W. M. (2015) Skin Deep: The Basics of Human Skin Structure and Drug Penetration, In *Percutaneous Penetration Enhancers Chemical Methods in Penetration Enhancement: Drug Manipulation Strategies and Vehicle Effects* (Dragicevic, N., and Maibach, H. I., Eds.), pp 3-11.

[6] Flaten, G. E., Bunjes, H., Luthman, K., and Brandl, M. (2006) Drug permeability across a phospholipid vesicle-based barrier 2. Characterization of barrier structure, storage stability and stability towards pH changes, *Eur J Pharm Sci 28*, 336-343.

[7] Puri, A., Murnane, K. S., Blough, B. E., and Banga, A. K. (2017) Effects of chemical and physical enhancement techniques on transdermal delivery of 3-fluoroamphetamine hydrochloride, *Int J Pharm 528*, 452-462.

[8] Pouillot, A., Dayan, N., Polla, A. S., Polla, L. L., and Polla, B. S. (2008) The stratum corneum: a double paradox, *J Cosmet Dermatol 7*, 143-148.

[9] Uchechi, O., Ogbonna, J. D. N., and Attama, A. A. (2014) Nanoparticles for Dermal and Transdermal Drug Delivery, In *Application of Nanotechnology in Drug Delivery*.

[10] Flaten, G. E., Palac, Z., Engesland, A., Filipovic-Grcic, J., Vanic, Z., and Skalko-Basnet, N. (2015) In vitro skin models as a tool in optimization of drug formulation, *Eur J Pharm Sci 75*, 10-24.

[11] Lee, S. H., Jeong, S. K., and Ahn, S. K. (2006) An update of the defensive barrier function of skin, *Yonsei Med J 47*, 293-306.

[12] Scheuplein, R. J., and Blank, I. H. (1971) Permeability of the skin, *Physiol Rev 51*, 702-747.

[13] Groen, D., Gooris, G. S., Ponec, M., and Bouwstra, J. A. (2008) Two new methods for preparing a unique stratum corneum substitute, *Biochim Biophys Acta 1778*, 2421-2429.

[14] Agache, P. (2004) Metrology of the stratum corneum, In *Measuring the skin: non-invasive investigations, physiology, normal constants*, pp 101-111.

[15] Fowler, J. (2012) Understanding the Role of Natural Moisturizing Factor in Skin Hydration, *Practical dermatology*.

[16] Walters, K. A., and Roberts, M. S. (2002) The Structure and Function of Skin, In *Dermatological and Transdermal Formulations*, pp 1-39.

[17] Reinertson, R. P., and Wheatley, V. R. (1959) Studies on the chemical composition of human epidermal lipids, *J Invest Dermatol 32*, 49-59.

[18] Van Smeden, J., Janssens, M., Gooris, G. S., and Bouwstra, J. A. (2014) The important role of stratum corneum lipids for the cutaneous barrier function, *Biochim Biophys Acta 1841*, 295-313.

[19] Mojumdar, E. H., Gooris, G. S., Groen, D., Barlow, D. J., Lawrence, M. J., Deme, B., and Bouwstra, J. A. (2016) Stratum corneum lipid matrix: Location of acyl ceramide and cholesterol in the unit cell of the long periodicity phase, *Biochim Biophys Acta 1858*, 1926-1934.

[20] Zbytovská, J., Kiselev, M. A., Funari, S. S., Garamus, V. M., Wartewig, S., Palát, K., and Neubert, R. (2008) Influence of cholesterol on the structure of stratum corneum lipid model membrane, *Colloids and Surfaces A: Physicochemical and Engineering Aspects 328*, 90-99.

[21] Bos, J. D., and Meinardi, M. M. (2000) The 500 Dalton rule for the skin penetration of chemical compounds and drugs, *Exp Dermatol 9*, 165-169.

[22] Egawa, M., Nomura, J., and Iwaki, H. (2010) The evaluation of the amount of cis- and trans-urocanic acid in the stratum corneum by Raman spectroscopy, *Photochem Photobiol Sci 9*, 730-733.

[23] Alkilani, A. Z., McCrudden, M. T., and Donnelly, R. F. (2015) Transdermal Drug Delivery: Innovative Pharmaceutical Developments Based on Disruption of the Barrier Properties of the stratum corneum, *Pharmaceutics 7*, 438-470.

[24] Forster, M., Bolzinger, M. A., Fessi, H., and Briancon, S. (2009) Topical delivery of cosmetics and drugs. Molecular aspects of percutaneous absorption and delivery, *Eur J Dermatol 19*, 309-323.

[25] Prausnitz, M. R., Mitragotri, S., and Langer, R. (2004) Current status and future potential of transdermal drug delivery, *Nat Rev Drug Discov 3*, 115-124.

[26] Ruela, A. L. M., Perissinato, A. G., Lino, M. E. d. S., Mudrik, P. S., and Pereira, G. R. (2016) Evaluation of skin absorption of drugs from topical and transdermal formulations, *Brazilian Journal of Pharmaceutical Sciences 52*, 527-544.

[27] Schaefer, U. F., Hansen, S., Schneider, M., Contreras, J. L., and Lehr, C. M. (2008) Models for Skin Absorption and Skin Toxicity Testing, In *Drug Absorption Studies*, pp 3-33.

[28] Van Gele, M., Geusens, B., Brochez, L., Speeckaert, R., and Lambert, J. (2011) Three-dimensional skin models as tools for transdermal drug delivery: challenges and limitations, *Expert Opin Drug Deliv 8*, 705-720.

[29] Abd, E., Yousef, S. A., Pastore, M. N., Telaprolu, K., Mohammed, Y. H., Namjoshi, S., Grice, J. E., and Roberts, M. S. (2016) Skin models for the testing of transdermal drugs, *Clin Pharmacol 8*, 163-176.

[30] Ponec, M. (1992) In vitro cultured human skin cells as alternatives to animals for skin irritancy screening, *Int J Cosmet Sci 14*, 245-264.

[31] Netzlaff, F., Lehr, C. M., Wertz, P. W., and Schaefer, U. F. (2005) The human epidermis models EpiSkin, SkinEthic and EpiDerm: an evaluation of morphology and their suitability for testing phototoxicity, irritancy, corrosivity, and substance transport, *Eur J Pharm Biopharm 60*, 167-178.

[32] Schafer-Korting, M., Bock, U., Diembeck, W., Dusing, H. J., Gamer, A., Haltner-Ukomadu, E., Hoffmann, C., Kaca, M., Kamp, H., Kersen, S., Kietzmann, M., Korting, H. C., Krachter, H. U., Lehr, C. M., Liebsch, M., Mehling, A., Muller-Goymann, C., Netzlaff, F., Niedorf, F., Rubbelke, M. K., Schafer, U., Schmidt, E., Schreiber, S., Spielmann, H., Vuia, A., and Weimer, M. (2008) The use of reconstructed human epidermis for skin absorption testing: Results of the validation study, *Altern Lab Anim 36*, 161-187.

[33] Oliveira, G., Beezer, A. E., Hadgraft, J., and Lane, M. E. (2011) Alcohol enhanced permeation in model membranes. Part II. Thermodynamic analysis of membrane partitioning, *Int J Pharm 420*, 216-222.

[34] Sinko, B., Garrigues, T. M., Balogh, G. T., Nagy, Z. K., Tsinman, O., Avdeef, A., and Takacs-Novak, K. (2012) Skin-PAMPA: a new method for fast prediction of skin penetration, *Eur J Pharm Sci 45*, 698-707.

[35] Engesland, A., Skar, M., Hansen, T., Skalko-Basnet, N., and Flaten, G. E. (2013) New applications of phospholipid vesicle-based permeation assay: permeation model mimicking skin barrier, *J Pharm Sci 102*, 1588-1600.

[36] Flaten, G. E., Dhanikula, A. B., Luthman, K., and Brandl, M. (2006) Drug permeability across a phospholipid vesicle based barrier: a novel approach for studying passive diffusion, *Eur J Pharm Sci 27*, 80-90.

[37] Flaten, G., Awoyemi, O., Luthman, K., Brandl, M., and Massing, U. (2009) The Phospholipid Vesicle-Based Drug Permeability Assay: 5. Development Toward an Automated Procedure for High-Throughput Permeability Screening, *Journal of the Association for Laboratory Automation 14*, 12-21.

[38] Palac, Z., Engesland, A., Flaten, G. E., Skalko-Basnet, N., Filipovic-Grcic, J., and Vanic, Z. (2014) Liposomes for (trans)dermal drug delivery: the skin-PVPA as a novel in vitro stratum corneum model in formulation development, *J Liposome Res 24*, 313-322.

[39] Engesland, A., Skalko-Basnet, N., and Flaten, G. E. (2015) Phospholipid vesicle-based permeation assay and EpiSkin(R) in assessment of drug therapies destined for skin administration, *J Pharm Sci 104*, 1119-1127.

[40] Li, J., Wang, X., Zhang, T., Wang, C., Huang, Z., Luo, X., and Deng, Y. (2015) A review on phospholipids and their main applications in drug delivery systems, *Asian Journal of Pharmaceutical Sciences 10*, 81-98.

[41] Zhang, H. (2017) Thin-Film Hydration Followed by Extrusion Method for Liposome Preparation, *Methods Mol Biol 1522*, 17-22.

[42] Abraham, W., and Downing, D. T. (1989) Preparation of model membranes for skin permeability studies using stratum corneum lipids, *J Invest Dermatol 93*, 809-813.

[43] Instruments, M. Dynamic Light Scattering - An Introduction in 30 Minutes, *Malvern Instruments Ltd.*

[44] Kobayashi, H., Ogawa, M., Alford, R., Choyke, P. L., and Urano, Y. (2010) New strategies for fluorescent probe design in medical diagnostic imaging, *Chem Rev 110*, 2620-2640.

[45] Félix, M. M., Umakoshi, H., Shimanouchi, T., Yoshimoto, M., and Kuboi, R. (2002) Evaluation of interaction between liposome membranes induced by stimuli responsive polymer and protein, *Journal of Bioscience and Bioengineering 93*, 498-501.

[46] Patel, H., Tscheka, C., and Heerklotz, H. (2009) Characterizing vesicle leakage by fluorescence lifetime measurements, *Soft Matter 5*, 2849.

[47] Shimanouchi, T., Ishii, H., Yoshimoto, N., Umakoshi, H., and Kuboi, R. (2009) Calcein permeation across phosphatidylcholine bilayer membrane: effects of membrane fluidity, liposome size, and immobilization, *Colloids Surf B Biointerfaces 73*, 156-160.

[48] Maherani, B., Arab-Tehrany, E., Kheirolomoom, A., Geny, D., and Linder, M. (2013) Calcein release behavior from liposomal bilayer; influence of physicochemical/mechanical/structural properties of lipids, *Biochimie 95*, 2018-2033.

[49] Ternullo, S., de Weerd, L., Flaten, G. E., Holsaeter, A. M., and Skalko-Basnet, N. (2017) The isolated perfused human skin flap model: A missing link in skin penetration studies?, *Eur J Pharm Sci 96*, 334-341.

[50] Gomes, M. J., Dreier, J., Brewer, J., Martins, S., Brandl, M., and Sarmento, B. (2016) A new approach for a blood-brain barrier model based on phospholipid vesicles: Membrane development and siRNA-loaded nanoparticles permeability, *Journal of Membrane Science 503*, 8-15.

[51] Zhu, C., Jiang, L., Chen, T. M., and Hwang, K. K. (2002) A comparative study of artificial membrane permeability assay for high throughput profiling of drug absorption potential, *Eur J Med Chem 37*, 399-407.

[52] Prankerd, R. J. (2007) Appendix A, *Profiles of Drug Substances, Excipients and Related Methodology 33*, 35-424.

[53] Swarbrick, J. (1987) Clarke's Isolation and Identification of Drugs, *Journal of Pharmaceutical Sciences 76*, 420-421.
[54] Luo, L., and Lane, M. E. (2015) Topical and transdermal delivery of caffeine, *Int J Pharm 490*, 155-164.
[55] Oliyai, R., and Stella, V. J. (1992) Kinetics and mechanism of isomerization of cyclosporin A, *Pharm Res 9*, 617-622.
[56] Nehlig, A., Daval, J. L., and Debry, G. (1992) Caffeine and the central nervous system: mechanisms of action, biochemical, metabolic and psychostimulant effects, *Brain Res Brain Res Rev 17*, 139-170.
[57] Herman, A., and Herman, A. P. (2013) Caffeine's mechanisms of action and its cosmetic use, *Skin Pharmacol Physiol 26*, 8-14.
[58] OECD. (2004) OECD guideline for the testing of chemicals. Skin absorption: in vitro method, No. 428 pp 1–8.
[59] Stuttgen, G. (1988) The present status of anti-inflammatory agents in dermatology, *Drugs 36 Suppl 5*, 43-48, discussion 49-50.
[60] Swart, H., Breytenbach, J. C., Hadgraft, J., and du Plessis, J. (2005) Synthesis and transdermal penetration of NSAID glycoside esters, *Int J Pharm 301*, 71-79.
[61] Heyneman, C. A., Lawless-Liday, C., and Wall, G. C. (2000) Oral versus topical NSAIDs in rheumatic diseases: a comparison, *Drugs 60*, 555-574.
[62] Bonina, F. P., Puglia, C., Barbuzzi, T., de Caprariis, P., Palagiano, F., Rimoli, M. G., and Saija, A. (2001) In vitro and in vivo evaluation of polyoxyethylene esters as dermal prodrugs of ketoprofen, naproxen and diclofenac, *European Journal of Pharmaceutical Sciences 14*, 123-134.
[63] Puglia, C., Blasi, P., Rizza, L., Schoubben, A., Bonina, F., Rossi, C., and Ricci, M. (2008) Lipid nanoparticles for prolonged topical delivery: an in vitro and in vivo investigation, *Int J Pharm 357*, 295-304.
[64] Patel, R. V., Clark, L. N., Lebwohl, M., and Weinberg, J. M. (2009) Treatments for psoriasis and the risk of malignancy, *J Am Acad Dermatol 60*, 1001-1017.
[65] Ferreira, M., Silva, E., Barreiros, L., Segundo, M. A., Costa Lima, S. A., and Reis, S. (2016) Methotrexate loaded lipid nanoparticles for topical management of skin-related diseases: Design, characterization and skin permeation potential, *Int J Pharm 512*, 14-21.
[66] Lopes, L. B., Collett, J. H., and Bentley, M. V. (2005) Topical delivery of cyclosporin A: an in vitro study using monoolein as a penetration enhancer, *Eur J Pharm Biopharm 60*, 25-30.
[67] Wakelin, S. H. (2017) Dermatological pharmacology: systemic drugs, *Medicine 45*, 363-367.
[68] Fischer, S. M., Flaten, G. E., Hagesaether, E., Fricker, G., and Brandl, M. (2011) In-vitro permeability of poorly water soluble drugs in the phospholipid vesicle-based permeation assay: the influence of nonionic surfactants, *J Pharm Pharmacol 63*, 1022-1030.
[69] Flaten, G. E., Luthman, K., Vasskog, T., and Brandl, M. (2008) Drug permeability across a phospholipid vesicle-based barrier 4. The effect of tensides, co-solvents and pH changes on barrier integrity and on drug permeability, *Eur J Pharm Sci 34*, 173-180.
[70] Simon, A., Amaro, M. I., Healy, A. M., Cabral, L. M., and de Sousa, V. P. (2016) Comparative evaluation of rivastigmine permeation from a transdermal system in the Franz cell using synthetic membranes and pig ear skin with in vivo-in vitro correlation, *Int J Pharm 512*, 234-241.
[71] Alves, A. C., Ramos, I. I., Nunes, C., Magalhaes, L. M., Sklenarova, H., Segundo, M. A., Lima, J. L., and Reis, S. (2016) On-line automated evaluation of lipid nanoparticles transdermal permeation using Franz diffusion cell and low-pressure chromatography, *Talanta 146*, 369-374.

[72] Rouser, G., Fleischer, S., and Yamamoto, A. (1970) Two dimensional thin layer chromatographic separation of polar lipids and determination of phospholipids by phosphorus analysis of spots, *Lipids 5*, 494-496.
[73] Berger, N., Sachse, A., Bender, J., Schubert, R., and Brandl, M. (2001) Filter extrusion of liposomes using different devices: comparison of liposome size, encapsulation efficiency, and process characteristics, *International Journal of Pharmaceutics 223*, 55-68.
[74] Hope, M. J., Nayar, R., Mayer, L.D., Cullins, P.R. (1993) Reduction of liposome size and preparation of unilamellar vesicles by extrusion techniques., *Liposome Technology, Liposome Preparation and Related Techniques, CSC Press, Boca Raton*, 124–139.
[75] Barrows, J. N., Jameson, G. B., and Pope, M. T. (1985) Structure of a heteropoly blue. The four-electron reduced .beta.-12-molybdophosphate anion, *Journal of the American Chemical Society 107*, 1771-1773.
[76] Fulton, T. B. (2009) Diffusion and Transport Across Cell Membranes, Prologue Course, University of California, Academy of Medical Educators, San Francisco, pp 65-85.
[77] Bucking, M., Gudgin Dickson, E. F., Farahani, M., Fischer, F., Holmes, D., Jori, G., Kennedy, J. C., Kenney, M. E., Peng, X., Pottier, R. H., and Weagle, G. (2000) Quantification of the selective retention of palladium octabutoxynaphthalocyanine, a potential photothermal drug, in mouse tissues, *J Photochem Photobiol B 58*, 87-93.
[78] Williams, A. C., and Barry, B. W. (2004) Penetration enhancers, *Adv Drug Deliv Rev 56*, 603-618.
[79] Elnaggar, Y. S., El-Massik, M. A., and Abdallah, O. Y. (2009) Self-nanoemulsifying drug delivery systems of tamoxifen citrate: design and optimization, *Int J Pharm 380*, 133-141.
[80] Menezes, A. C., Campos, P. M., Euleterio, C., Simoes, S., Praca, F. S., Bentley, M. V., and Ascenso, A. (2016) Development and characterization of novel 1-(1-Naphthyl)piperazine-loaded lipid vesicles for prevention of UV-induced skin inflammation, *Eur J Pharm Biopharm 104*, 101-109.
[81] Tanojo, H., Bos-van Geest, A., Bouwstra, J. A., Junginger, H. E., and Boodé, H. E. (1997) In vitro human skin barrier perturbation by oleic acid: Thermal analysis and freeze fracture electron microscopy studies, *Thermochimica Acta 293*, 77-85.
[82] Nerurkar, M. M., Ho, N. F., Burton, P. S., Vidmar, T. J., and Borchardt, R. T. (1997) Mechanistic roles of neutral surfactants on concurrent polarized and passive membrane transport of a model peptide in Caco-2 cells, *J Pharm Sci 86*, 813-821.
[83] Jewell, C., Heylings, J., Clowes, H. M., and Williams, F. M. (2000) Percutaneous absorption and metabolism of dinitrochlorobenzene in vitro, *Arch Toxicol 74*, 356-365.